Time-based redeployment of multi-class nodes for reliable wireless sensor network coverage

Nayan Chakrabarty¹, Kelly M. Sullivan¹, and Daniel B. Lopes da Silva²

¹Department of Industrial Engineering, University of Arkansas, Fayetteville, AR, USA, 72701 ²Department of Industrial Engineering, Clemson University, Clemson, SC, USA, 29634

Abstract

We consider the problem of redeploying nodes into a wireless sensor network (WSN) to maintain reliable area coverage over time as nodes fail. Specifically, we consider the class of time-based node redeployment policies in which the WSN is inspected after a fixed amount of time, after which new sensor nodes are redeployed to bring the number of functioning nodes to a desired level. Whereas previous research on time-based node redeployment assumes nodes are identical with respect to time to failure, we use multiple classes of sensor nodes to represent a scenario where nodes' times to failure are dependent on positioning in the network. We propose a partial survival signature (PSS) approach for estimating area coverage reliability under a given time-based redeployment policy, where the PSS is estimated by Monte Carlo simulation. This PSS representation enables efficient re-evaluation of coverage reliability under different redeployment policies, thus allowing the use of metaheuristics to obtain a set of redeployment policies that are near-efficient with respect to cost and coverage reliability. We present a numerical example to demonstrate that the PSS approach yields accurate estimates of coverage reliability within a reasonable amount of computation time. Furthermore, we apply non-dominated sorting genetic algorithm II (NSGA-II) to optimize the numerical example with respect to cost and coverage reliability.

Acknowledgments

This material is based upon work supported by the National Science Foundation under Grant No. CMMI-1751191. This work was conducted fully or in part on computational resources at the Arkansas High Performance Computing Center

1 Introduction

Wireless sensor networks (WSNs) have received substantial attention in the literature due to their wide applications, including military, health care, and infrastructure environment monitoring. A WSN is a collection of sensor nodes that can record and transmit data through the network to monitor a region or system of interest. WSNs present an attractive alternative to wired monitoring systems due to their low cost and flexibility of deployment. Conceptually, a large number of low-cost sensor nodes can work together to record data over a substantial area, and for a significant duration of time; however, it is challenging to deploy WSNs at scale for a number of reasons, one of which is the potential for node failure, either due to hardware malfunction or exhaustion of a limited power supply for required communicating, processing, and sensing tasks [1].

In practice, the occurrence of node failures may be uncertain due to unpredictable environmental conditions and inherent difficulties in predicting the lifetime of sensor node batteries [2, 3]. Considering this uncertainty, substantial research has focused on characterizing WSN performance with respect to a variety of network reliability metrics as well as improving WSN reliability through design and control strategies.

One way to improve the reliability of a WSN with uncertain node failures is by periodically deploying new nodes into the WSN. These actions can be costly, especially when the WSN is deployed in an area that is difficult to access. It is therefore of interest to determine cost-efficient policies for deploying new WSN nodes (e.g., including the quantity and location of nodes and timing of deployment) to improve WSN reliability. This problem is challenging in general due to sequential and dynamic nature of decisions as well as the underlying difficulty in evaluating WSN reliability metrics.

In this work, we consider the problem of redeploying unreliable sensor nodes periodically into a multi-hop WSN to maximize the WSN's α -coverage reliability (i.e., the probability that the WSN covers at least a threshold proportion of target nodes) while also minimizing the cost rate due to deploying nodes. We consider node deployment policies that allow for specifying the quantity of

nodes to deploy and the frequency of redeployment. Although the location of deployed nodes is assumed to be random, the policies also allow for controlling the extent to which sensor nodes are centrally concentrated near the sink node, similar to [4]. It is well known that nodes located near the sink node are more heavily utilized to relay communications, thus resulting in faster battery consumption and shorter lifetimes. We incorporate this feature by grouping sensor nodes into classes based on distance from the sink node and assuming nodes within each class share a common time-to-failure distribution.

The contributions of this work follow:

- 1. To our knowledge, this paper is the first to examine the problem of reliable multi-hop WSN node redeployment in the context of load-heterogeneous nodes.
- 2. We formalize the concept of a time-based node redeployment policy in the context of nodes with position-dependent time to failure.
- 3. Using survival signatures, we characterize a WSN's α-coverage reliability under a given time-based node redeployment policy. This characterization disaggregates computational complexity arising due to design decisions (e.g., the size of the network) and redeployment frequency, thus enabling exploration of time-based node redeployment policies that are efficient with respect to cost and area coverage reliability.
- 4. We propose a Monte Carlo approach (MC) for estimating α-coverage reliability based upon estimating only a portion of the survival signature elements. The proposed *partial survival signature* (PSS) estimation enables quickly reevaluating α-coverage reliability for networks with more than two node classes. To the best of our knowledge, our work is the first to estimate a system's reliability by using a PSS. Due to the computational complexity associated with evaluating the full survival signature, this contribution may enable enhanced reliability estimation procedures for other large-scale systems.

The proposed method for estimating α -coverage reliability is advantageous because MC need only be performed once (to estimate the PSS) for each problem instance. This PSS estimate can be

reused to estimate the α -coverage reliability of different time-based node redeployment policies, thereby reducing computational effort associated with policy exploration. By contrast, although it is also possible to estimate α -coverage reliability using other sophisticated MC approaches (e.g., Lomonosov's Turnip [5, Chapter 9]), doing so would require performing MC once for each time-based node redeployment policy explored.

Below, we summarize our main assumptions, which are defined formally in Section 4:

- 1. The sink node and all target nodes are perfectly reliable.
- 2. Communications are distance-based. That is, a sensor node can (with perfect reliability) communicate with other nodes or monitor a target node located within a predefined distance.
- 3. Sensor nodes in the same class have identical time-to-failure distribution.
- 4. Sensor nodes are independent with respect to failure time.
- 5. Sensor nodes are deployed randomly.

The remainder of this paper is organized as follows. Section 2 summarizes the literature related to our research. Section 3 provides an overview of survival signature followed by a formal introduction of the WSN model and α -coverage reliability metric in Section 4. Section 5 provides a general characterization of α -coverage reliability using the survival signature. Section 5 introduces the PSS and presents methodology for estimating α -coverage reliability through MC simulation of the PSS. Section 6 demonstrates the results through several examples.

2 Literature Review

In what follows, we review the literature related to our contributions. Specifically, our research investigates WSN node redeployment policies with respect to a network reliability metric; therefore, this section highlights previous works related to WSN node deployment and redeployment as well as WSN reliability. In subsection 2.1, we review the literature related to WSN node deployment

and redeployment strategies, and we categorize the papers based on the metrics or restrictions used to guide (re)deployment of nodes. In subsection 2.2, we summarize papers focused on evaluating and improving WSN reliability and explain the relation to our work.

2.1 WSN Node Deployment and Redeployment

Substantial research has focused on determining the initial location of WSN nodes while considering the impact on WSN lifetime and performance.

With regard to WSN lifetime, node location is an important design consideration because sensor nodes close to the sink node are known to have a heavier traffic load and thus have a shorter lifetime. Researchers have examined a variety of random deployment strategies and noted that non-uniform deployment of sensor nodes enable achieving more balanced energy consumption among the WSN nodes [6], potentially improving the network's capacity or prolonging the WSN's lifetime. Chang and Chang [7] proposed a node placement technique in which the region of interest is partitioned into zones and then the number of nodes to be deployed (randomly) within each region is determined using distance and density considerations. Researchers have also sought to improve network lifetime by deploying sensor nodes randomly according to a Gaussian [4, 8] and other non-uniform distributions [9, 10, 11]. Other researchers have examined deterministic layouts [12, 13] designed to create redundant sensor-to-sink paths. Whereas many of these works focus on locating sensor nodes, researchers have also sought to extend network lifetime by strategically placing higher-powered relay nodes specifically designed to assume some of the burden of communicating data toward the sink node [14, 15, 16]. In addition to node location decisions, the research summarized in this paragraph has sought to extend network lifetime by jointly considering topology control [6], routing [10, 11, 16], and clustering [7, 8, 13] decisions.

Many works in the literature have sought to identify WSN node deployment strategies that ensure *coverage* (i.e., all targets can be monitored by a sensor node) and *network connectivity* [17] (i.e., all sensor nodes can communicate with each other and/or sink nodes). A heuristic sensor deployment algorithm, where sensor nodes can be relocated after initial deployment, is proposed

in [18] to ensure coverage. Yu et al. [19] examine a related problem in which a minimum subset of sensor node locations is chosen while ensuring k-coverage, in which each target should be monitored by at least k > 1 sensor nodes. Misra et al. [20] and Almasaeid and Kamal [21] examine the problem of placing a minimum number of relay nodes to ensure k-connectivity, in which sensor nodes are connected to the sink node by at least k > 1 node-disjoint paths. Researchers have also focused on combining both coverage and connectivity in the objectives to decide on node deployment. For example, the authors in [22, 23] proposed multi-objective optimization models for sensor node deployment in WSNs, which considered objectives such as the number of sensor nodes, coverage, connectivity, and energy consumption. Although the works summarized in this paragraph may enable increasing a WSN's tolerance to component failures, they do not directly model uncertainty in component failures.

In addition to sensor node deployment, researchers have also examined sensor node replacement policies after initial deployment. Node replacement strategies were proposed in [24, 25] where a mobile robot or human periodically travels the network to determine which nodes should be replaced and replace those with new one. References [26] and [27] developed node redeployment policies where the decision of replacing a failed node depends on the importance of this node on the sensing coverage, and reference [28] proposed a joint routing and node deployment policy to minimize the deployment cost. These papers on node replacement do not directly address WSN reliability when determining node replacement.

2.2 WSN Reliability

Although early researchers noted the need for WSNs to have reliable "sensor-to-sink" and "event-to-sink" communications [29, 30], the work of AboElFotoh et al. [31, 32] appears to be the first work to characterize a network-wide WSN reliability measure. This initial network reliability measure, which was characterized for a WSN with cluster-based architecture and (independent) unreliable nodes, was later extended to incorporate common-cause failure [33, 34, 35].

A variety of network reliability measures have been applied to WSNs. For example, research

has considered WSN reliability measures based on two-terminal reliability [36, 37], *k*-terminal reliability [38, 39], and all-terminal reliability [40, 41]. Researchers have examined WSN reliability in the presence of unreliable nodes [42, 43, 44, 45] as well as unreliable transmission of data [46, 47]. With some exceptions, these works primarily focus only on evaluating a WSN's reliability. A variety of methods have been used for evaluating WSN reliability. Factoring [31, 42], sum of disjoint products [45, 48], and binary decision diagrams [33, 34] are the most common exact methods that have been used to evaluate WSN reliability. Due to the complexity of evaluating exactly, Monte-Carlo simulation has also been used extensively to estimate WSN reliability [43, 49, 50, 51, 52].

A number of researchers have sought to improve or optimize WSN reliability by determining initial number and arrangement of number of sensor nodes or controlling WSN operations. For example, Xiang and Yang [51] proposed a design based on determining the minimum number of sensors needed to ensure a desired level of coverage reliability. Khoshraftar and Heidari [53] applied a genetic algorithm to improve the construction of clusters (for hierarchical routing of data) with respect to a network reliability measure. A variety of other metaheuristics have been applied to optimize WSN reliability, including the social spider algorithm [54], particle swarm optimization [55], and ant colony optimization [56]. In recent studies, researchers have also sought to improve WSNs with respect to data transmission reliability by scheduling data retransmissions on network links [57], scheduling sensor nodes in sleep/wake states [58], and prioritizing urgent "real-time" packets to manage packet congestion at nodes [59]. The papers discussed in this paragraph do not consider the possibility of adding nodes to the WSN to prolong functionality beyond an initial mission.

With respect to a WSN with linear consecutive (r,s)-out-of-(m,n): F structure, Zhang et al [60] propose two methods to analyze WSN reliability in the presence of repairable nodes. Similarly focusing on linear WSNs, researchers have analyzed preventive maintenance schedules [61], sensor node allocation policies [62], and transmission power and data packet size assignment strategies [63]. In comparison to the papers summarized in this paragraph, our work does not assume any

special structure of the WSN topology.

To our knowledge, there is little previous research that aims to identify node deployment and redeployment strategies that are efficient with respect to both a WSN reliability measure and sensor deployment cost. Lin et al. [64] introduce the problem of identifying a cost-optimal age-based redeployment policies for a WSN with unreliable nodes. This initial problem assumes the WSN has single-hop (i.e., *star*) topology and that surviving nodes cannot be carried over for use after deploying new nodes. Deif and Gadallah [56] applied ant colony optimization to minimize sensor deployment cost while maintaining a predefined minimum level of WSN reliability. Chen et al. [65] developed a multi-objective sensor deployment optimization model to maximize WSN reliability, measured by coverage and connection degree, while minimizing sensor deployment cost. Neither [56] nor [65] consider the possibility of redeploying nodes restore the WSN's functionality after nodes have failed.

Our research is most closely related to the work of Boardman and Sullivan [66], which characterizes the α -coverage reliability and cost rate of a WSN with random node position under a given time-based node redeployment schedule. Boardman and Sullivan [66] utilize a destruction-spectrum-based representation of α -coverage reliability that allows quick re-evaluation of redeployment policies. This initial work was later extended to explore condition-based redeployment policies in which node redeployment actions are triggered based upon the state of the network instead of by a fixed schedule [67, 68]. A limitation of these works is that they assume nodes are independent and identically distributed (i.i.d.) with respect to time-to-failure distribution. Here, we extend this work to the case of multiple classes of sensor nodes, each of which is characterized by a different time-to-failure distribution. We associate the sensor node classes with different sub regions of the WSN, thus capturing a scenario where sensor node deployed close to the sink node are prone to fail more quickly than sensor nodes deployed far from sink node.

3 Overview of Survival Signature

In what follows, we provide a brief summary of methodology for characterizing system reliability based on the survival signature, which was introduced by [69] to characterize the reliability of a complex system with multiple classes of binary-state (i.e., functioning or non-functioning) components. Because this methodology can be applied to a variety of systems (i.e., not only networks), we use the term *system reliability* in this section. Later, we explain in Section 5 how we incorporate the survival signature to characterize α -coverage reliability.

Consider a system consisting of $K \ge 2$ classes of components in which components of the same class are assumed to have i.i.d. time to failure while components of different classes are assumed to be independent but not identical with respect to time to failure. Let $F_k(t)$, t > 0, denote the shared time-to-failure cumulative distribution function (c.d.f.) of components in class k = 1, 2, ..., K and define T > 0 as the system's time to failure.

Let n_k denote the number of components in class $k=1,\ldots,K$, and define $n=\sum_{k=1}^K n_k$ as the number of components in the system. Let the state vector associated with class $k=1,\ldots,K$ be given by $x^k=(x_1^k,x_2^k,\ldots,x_{n_k}^k)$, where $x_i^k=1$ if the *i*th component in class k is functional and $x_i^k=0$ otherwise, and define the system state vector as $x=(x^1,x^2,\ldots,x^K)$. Let $S_l^k=\{0,1\}^{n_k}$ denote the set of potential state vectors associated with class k, and define $S_l=S_l^1\times S_l^2\times\cdots\times S_l^K$ as the set of potential system state vectors. Define the system structure function $\psi(x)$, which equals 1 if the system is functioning in state $x\in S_l$ and 0 otherwise.

Let $\phi(l_1, l_2, \dots, l_K)$ denote the probability the system functions given that exactly $l_k \in \{0, 1, \dots, n_k\}$ of its class k components function, for each $k = 1, 2, \dots, K$. As shown by Coolen and Coolen-Maturi [69], conditioning on (l_1, l_2, \dots, l_K) enables characterizing the system's reliability P(T > t) at time t > 0 as

$$P(T > t) = \sum_{l_1=0}^{n_1} \sum_{l_2=0}^{n_2} \cdots \sum_{l_k=0}^{n_k} \phi(l_1, l_2, \dots, l_K) \prod_{k=1}^K \left(\binom{n_k}{l_k} [F_k(t)]^{n_k - l_k} [1 - F_k(t)]^{l_k} \right). \tag{1}$$

The collection of values $\phi(l_1, l_2, \dots, l_K)$ is referred to as the *survival signature*. Computing the survival signature is complex as it requires calculating $\prod_{k=1}^{K} (n_k + 1)$ elements, each of which requires counting the (potentially exponential) number of system state vectors in which the system is functioning and a given number of components function in each class. However, the survival signature has certain benefits over traditional methods. For instance, it has the ability to separate the system structure from the probabilistic information. Although exact methods have been developed for evaluating a system's survival signature [70, 71, 72], it is common to estimate the survival signature of large-scale systems using Monte Carlo simulation [73, 74, 75].

4 WSN Model and Definition of α -Coverage Reliability

In this research, we examine the problem of periodically redeploying sensor nodes into a region \mathcal{R} to ensure a high probability of area coverage. Mathematically we model the WSN as a network with a single sink node 0, sensor nodes \mathcal{N} , and target nodes \mathcal{T} . Here, the purpose of the target nodes is to provide a discrete representation of the area that needs to be covered. In the case of multiple sink nodes, without loss of generality, one can model the network by introducing an artificial node 0 adjacent to each of the sink nodes.

We assume a disk graph model wherein each sensor node can communicate with any other sensor node located within a distance of $d_1 > 0$ and monitor any target node located within a distance of $d_2 > 0$. Define the directed arc set $\mathcal{A}^{\text{com}} \subseteq (\mathcal{N} \cup \{0\}) \times \mathcal{N}$ to represent the set of ordered node pairs (i,j) such that sensor (or sink) node $i \in (\mathcal{N} \cup \{0\})$ is within a distance d_1 of (and can communicate with) sensor node $j \in \mathcal{N}$. Let $\mathcal{A}^{\text{mon}} \subseteq \mathcal{N} \times \mathcal{T}$ denote a set of directed arcs that contains the sensor-target node pairs (i,j) if target node $j \in \mathcal{T}$ can be monitored by sensor node i. Let $\mathcal{G} = (\mathcal{M}, \mathcal{A})$ denote the resulting directed network with nodes $\mathcal{M} = \mathcal{N} \cup \{0\} \cup \mathcal{T}$ and directed arcs $\mathcal{A} = \mathcal{A}^{\text{com}} \cup \mathcal{A}^{\text{mon}}$. A target node $j \in \mathcal{T}$ is said to be *covered* if \mathcal{G} contains a directed path from the sink node 0 to j, and the *coverage* of \mathcal{G} is the proportion of target nodes covered.

As we summarize in the following paragraphs, the network G evolves stochastically over time

as sensor nodes fail or are added to the network; therefore, denote the network at time t > 0 by $\mathcal{G}(t)$, and let $C[\mathcal{G}(t)]$ denote the coverage of $\mathcal{G}(t)$. For a given threshold α , $0 \le \alpha \le 1$, we define the network as functioning if $C[\mathcal{G}(t)] \ge \alpha$ and failed otherwise. We are concerned with designing cost-efficient redeployment policies to ensure the α -coverage reliability

$$R(t) = \Pr\{C[\mathcal{G}(t)] \ge \alpha\} \tag{2}$$

remains high as the network evolves.

The sensor nodes \mathcal{N} are assumed to be divided into K classes (i.e., subsets) \mathcal{N}_1 , \mathcal{N}_2 , ..., \mathcal{N}_K such that the sensor nodes within each class have i.i.d. time-to-failure distribution. Whereas the prior work of Boardman and Sullivan [66] assumes all nodes have i.i.d. time to failure, utilizing multiple classes of nodes allows for modeling a scenario where nodes experience different loads and therefore have varying time-to-failure distributions. In practice, heterogeneous loads could be caused as a result of the well-known energy-hole problem [76, 77, 78, 79, 80], which arises because nodes closer to the sink are more heavily relied upon to transmit data. Alternatively, nodes could experience different time-to-failure distributions due to different hardware components or varying environmental conditions.

In accordance with the above, we assume a sensor node's class (and thus its time-to-failure distribution) depends on where it is located within the region \mathcal{R} . Specifically, we assume \mathcal{R} is partitioned into K subregions, i.e., $\mathcal{R} = \mathcal{R}_1 \cup \mathcal{R}_2 \cup \cdots \cup \mathcal{R}_K$, such that nodes in $\mathcal{N}_1, \mathcal{N}_2, \ldots, \mathcal{N}_K$ are respectively located in $\mathcal{R}_1, \mathcal{R}_2, \ldots, \mathcal{R}_K$.

In what follows, we summarize the assumed process by which the network evolves over time. Section 4.1 characterizes the assumed node-failure process and Section 4.2 follows by describing time-based policies for redeploying nodes into the network

4.1 Node Failure Process

Let $F_k(t)$ denote the time-to-failure c.d.f. for nodes in \mathcal{N}_k , $\forall k = 1, 2, ..., K$. We make the following assumptions with regard to node failures.

Assumption 1. For each class k = 1, 2, ..., K, the nodes deployed in \mathcal{R}_k have i.i.d. time-to-failure distribution characterized by the c.d.f. $F_k(t)$.

Whereas Assumption 1 assumes both independence and a common time-to-failure c.d.f. among nodes within the same class, we also assume independence among nodes from different classes. This assumption is formalized below.

Assumption 2. Any subset of nodes deployed in $\mathcal{R}_1 \cup \mathcal{R}_2 \cup \cdots \cup \mathcal{R}_K$ is independent with respect to time-to-failure distribution.

We make the following additional simplifying assumption.

Assumption 3. The target nodes $j \in T$ and sink node 0 are completely reliable.

Although Assumption 3 imposes some loss of generality, note that the case of unreliable sink nodes could be modeled in a similar framework through including the sink node (0) within a dedicated node class.

4.2 Time-Based Node Deployment

In what follows, we summarize the assumed $(n_1, n_2, ..., n_K; t')$ time-based deployment policy, hereafter abbreviated as $(n_1, n_2, ..., n_K; t')$ -TBDP, by which new sensor nodes are added to the network. In this policy, n_k sensor nodes are initially deployed (i.e., at time 0) within \mathcal{R}_k . The following assumption governs the locations of deployed sensor nodes.

Assumption 4. New sensor nodes from class k are deployed randomly (and independently) with uniform density over \mathcal{R}_k , $\forall k = 1, 2, ..., K$.

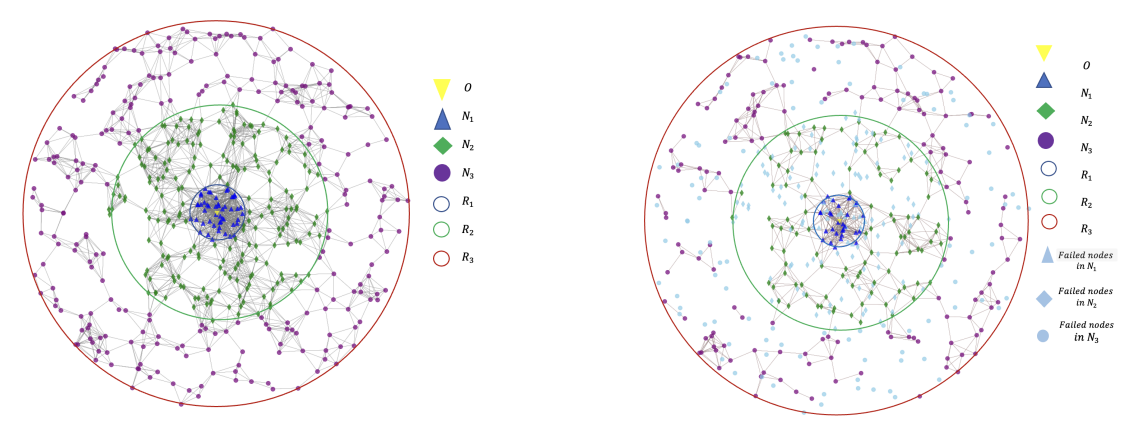


Figure 1: With all functioning sensor nodes Figure 2: After the failure of some sensor nodes

We define the term " $(n_1, n_2, ..., n_K)$ random geometric graph", hereafter abbreviated as $(n_1, n_2, ..., n_K)$ RGG, to refer to a network in which n_k nodes are randomly deployed into \mathcal{R}_k , $\forall k = 1, 2, ..., K$ according to Assumption 4.

Every t'>0 time units (i.e., at times ut', $u\in\mathbb{Z}_{>0}$) in the $(n_1,n_2,\ldots,n_K;t')$ -TBDP, the network is inspected and new nodes from class k are respectively added to \mathcal{R}_k to bring the number of functioning nodes in \mathcal{R}_k to n_k , $\forall k=1,2,\ldots,K$. The locations of nodes added in stage are also assumed to be governed by Assumption 4; thus, the network immediately after inspection is an (n_1,n_2,\ldots,n_K) -RGG. We summarize this property below.

Property 1. Under an $(n_1, n_2, ..., n_K; t')$ -TBDP, each network $\mathcal{G}(ut')$, $u \in \mathbb{Z}_{\geq 0}$ is an $(n_1, n_2, ..., n_K)$ -RGG.

Figures 1–3 illustrate an $(n_1, n_2, n_3; t')$ -TBDP for an example network. The regions \mathcal{R}_1 , \mathcal{R}_2 , and \mathcal{R}_3 are depicted as concentric disks centered around the sink node 0. Initially, $n_1 = 50$, $n_2 = 200$, and $n_3 = 250$ sensor nodes are randomly deployed in regions \mathcal{R}_1 , \mathcal{R}_2 , and \mathcal{R}_3 , respectively, as illustrated in Figure 1. Since sensor nodes randomly fail over time, we display in Figure 2 a scenario where 20 sensor nodes from \mathcal{N}_1 , 110 sensor nodes from \mathcal{N}_2 , and 133 sensor nodes from \mathcal{N}_3 have failed after the time interval t'. Figure 3 illustrates the replacement of failed sensor nodes from \mathcal{N}_1 , \mathcal{N}_2 , and \mathcal{N}_3 with new sensor nodes after t' to ensure that a total number of functioning sensor nodes for n_1, n_2 , and n_3 is achieved.

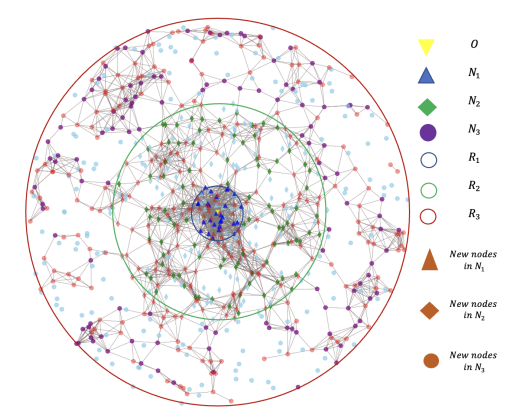


Figure 3: After adding new sensor nodes to $\mathcal{R}_1, \mathcal{R}_2$, and \mathcal{R}_3

5 Characterizing α -Coverage Reliability

After deploying new sensor nodes in an $(n_1, n_2, ..., n_K)$ -TBDP, the functioning sensor nodes will have different ages and residual lifetime distributions depending on when they were deployed. In what follows, we characterize a representation of α -coverage reliability after sensor node ages have reached stationarity. The analysis follows closely to [66] and is inspired by the results from [81].

Because the following analysis applies separately to sensor nodes from each class, we temporarily drop the "class" subscript for brevity of exposition. That is, suppose there is only one class of sensor nodes. Let $T \geq 0$ denote the lifetime of a sensor node, define F(t) as the c.d.f. of T, and define $\bar{F}(t) = 1 - F(t)$. Consider a sequence of *epochs* $u \in \mathbb{Z}_{\geq 0}$, where the uth epoch refers to the time interval ((u-1)t',ut']; thus, immediately after the uth epoch, the age X(u) of a sensor node is a random variable with range $\{ut': u \in \mathbb{Z}_{\geq 0}\}$. Furthermore, the stochastic process $\{X(u): u \in \mathbb{Z}_{\geq 0}\}$ is an infinite-horizon, discrete-time Markov chain with countably infinite states $u \in \mathbb{Z}_{\geq 0}$, where state u represents a sensor node having age equal to ut'. A sensor node with age ut' either survives the next epoch (with probability $\bar{F}((u+1)t')/\bar{F}(ut')$) or fails and is replaced by a new sensor; therefore, state u transitions to either state u+1 (with probability $\bar{F}((u+1)t')/\bar{F}(ut')$) or state 0 (with probability $(1-(\bar{F}((u+1)t')))/\bar{F}(ut')$). This Markov chain has the stationary

distribution

$$\Pr\left(X = ut'\right) = \frac{\bar{F}\left(ut'\right)}{\sum_{j=0}^{\infty} \bar{F}\left(jt'\right)},\tag{3}$$

provided that the denominator converges. A derivation of Equation (3) is provided in Appendix A.

Now consider a class of nodes, each described by a common time-to-failure c.d.f. F(t) and having random age X described by the probability distribution in Equation (3). This scenario describes each node class immediately after new nodes are deployed, assuming node ages have reached stationarity. A sensor node having age X = x has a residual lifetime $T_x \ge 0$ described by the c.d.f. $H_x(t) = (F(x+t) - F(x))/\bar{F}(x)$. By conditioning on X, the residual lifetime of a node with random age has c.d.f.

$$G(t;t') = \Pr(T_X \le t) = \sum_{u=0}^{\infty} \Pr(T_X \le t | X = ut') \Pr(X = ut')$$
(4a)

$$= \sum_{u=0}^{\infty} H_{ut'}(t) \operatorname{Pr}(X = ut')$$
(4b)

$$=\sum_{u=0}^{\infty} \frac{F(ut'+t) - F(ut')}{\bar{F}(ut')} \Pr(X = ut'), \tag{4c}$$

$$=\frac{\sum_{u=0}^{\infty}\left(F\left(ut'+t\right)-F\left(ut'\right)\right)}{\sum_{i=0}^{\infty}\bar{F}\left(jt'\right)}.$$
(4d)

The analysis above holds separately for each node class. Therefore we have that

$$G_k(t;t') = \frac{\sum_{u=0}^{\infty} F_k(ut'+t) - F_k(ut')}{\sum_{j=0}^{\infty} \bar{F}_k(jt')}, \qquad k = 1, 2, \dots, K.$$
 (5)

where $G_k(t;t')$ is the probability that a sensor node from class k selected at random after new deployment, survives an additional t time units. By applying Equation (1), the α -coverage reliability after redeployment can be expressed as

$$R(n_1, n_2, \dots, n_K; t; t') = \sum_{l_1=0}^{n_1} \sum_{l_2=0}^{n_2} \cdots \sum_{l_K=0}^{n_K} \phi(l_1, l_2, \dots, l_K) \prod_{k=1}^K b(l_k, n_k, 1 - G_k(t; t'))).$$
 (6)

where $\phi(l_1, l_2, \dots, l_K)$ is the probability that the network satisfies the coverage requirement given

that exactly l_k nodes from each class $k=1,2,\ldots,K$, are active. Here, b(l,n,p) represents the binomial probability function, i.e., $b(l,n,p)=\binom{n}{l}p^l(1-p)^{n-l}$. Note that $\phi(l_1,l_2,\ldots,l_K),\ l_k=0,1,\ldots,n_k,\ \forall\ k=1,2,\ldots,K$ are the *elements* of survival signature and that we refer to the corresponding $(n_1+1)\times(n_2+2)\times\cdots\times(n_K+1)$ matrix by Φ .

An advantage of this representation is that the survival signature is not dependent on the redeployment frequency t'; therefore, if the survival signature is computed (or estimated) for a single value of $(n_1, n_2, ..., n_K)$, Equation (6) can be used to quickly reevaluate α -coverage reliability for different redeployment frequencies t'.

6 Estimating α-Coverage Reliability

As the number of node classes K increases, it becomes prohibitive to store the full survival signature in memory, let alone to compute it (exactly) to evaluate α -coverage reliability using Equation (6). Here, we propose to estimate α -coverage reliability by performing Monte Carlo estimation of a portion of the $\prod_{k=1}^K (n_k+1)$ elements of Φ . Let $\mathcal{S} = \{(l_1^e, l_2^e, \dots, l_m^e)\}_{e=1}^E$ denote a multiset consisting of elements from $\{0, 1, \dots, n_1\} \times \{0, 1, \dots, n_2\} \times \dots \times \{0, 1, \dots, n_K\}$ and drawn at random with replacement, and with each element equally likely to be drawn. We estimate the α -coverage reliability as

$$\hat{R}(n_1, n_2, \dots, n_K; t; t') = \frac{\sum_{e=1}^{E} \phi(l_1^e, l_2^e, \dots, l_K^e) \prod_{k=1}^{K} b(l_k^e, n_k^e, 1 - G_k(t; t'))}{\sum_{e=1}^{E} \prod_{k=1}^{K} b(l_k^e, n_k^e, 1 - G_k(t; t'))}.$$
(7)

We define $\{\phi(l_1^e, l_2^e, \dots, l_K^e)\}_{e=1}^E$ as the *partial survival signature* (PSS) and refer to it henceforth using the notation Φ' . Correspondingly, we refer to \hat{R} defined in Equation (7) as PSS estimate of α -coverage reliability. We focus on the stable α -coverage reliability just before redeploying new sensor nodes, i.e., at time t=t'. Thus, we use t=t' in Equation (7) to evaluate α -coverage reliability.

When S contains exactly one copy of each element in $\{0,1,\ldots,n_1\} \times \{0,1,\ldots,n_2\} \times \cdots \times \{0,1,\ldots,n_K\}$, note that Equation (7) reduces to Equation (6), i.e., the PSS estimate is exact. To

summarize the intuition behind Equation (7), note that Equation (6) can be interpreted as an expression for $R(n_1, \ldots, n_K; t; t') = \mathbb{E}[\phi(L_1, L_2, \ldots, L_K)]$ by conditioning on the value of (L_1, L_2, \ldots, L_K) , where (L_1, L_2, \ldots, L_K) are independent and $L_k \sim \text{binom}(n_k, 1 - G_k(t; t'))$ for each $k = 1, 2, \ldots, K$. In Equation (6), $\prod_{k=1}^K (n_k + 1)$ terms are summed to yield $\mathbb{E}[\phi(L_1, L_2, \ldots, L_K)]$ using the probability mass function $h(l_1, l_2, \ldots, l_K) \equiv \prod_{k=1}^K b(l_k, n_k, 1 - G_k(t; t'))$. The PSS estimate replaces the $\prod_{k=1}^K (n_k + 1)$ -element outcome space of (L_1, L_2, \ldots, L_K) in Equation (6) with the multiset S, where $|S| < \prod_{k=1}^K (n_k + 1)$, in Equation (7). Because $p(S) \equiv \sum_{e=1}^E \prod_{k=1}^K b(l_k^e, n_k^e, 1 - G_k(t; t'))$ cannot be guaranteed to equal $1, h(l_1^e, l_2^e, \ldots, l_K^e)$ no longer represents a probability mass function on S; therefore, we replace $h(l_1, l_2, \ldots, l_K)$ in Equation (6) with $h(l_1^e, l_2^e, \ldots, l_K^e)/p(S)$ in Equation (7). Section 7.1 presents an empirical comparison of the PSS estimate relative to alternative methods for evaluating α -coverage reliability and demonstrates the PSS is competitive with respect to speed and estimation error.

Although Equation (7) alleviates the computational complexity due to the number of elements of Φ , it remains intractable to compute the elements of the PSS Φ' . With this motivation, Algorithm 1 presents a MC algorithm for estimating the PSS Φ' with respect to the collection of (n_1, n_2, \ldots, n_K) -RGGs. According to Assumption 1, sensor nodes in the same class have *i.i.d.* time-to-failure distribution; therefore, sensor nodes are equally likely to fail in any order. As implied by the Assumption 2, the sensor nodes in different classes are independent of each other. Therefore, we estimate Φ' by repeatedly sampling an (n_1, n_2, \ldots, n_K) -RGG and K independent permutations specifying the order of failure of nodes within each class.

Step 1 accepts input specifying the size of the network (i.e., the number of nodes n_k located in each region \mathcal{R}_k , $k=1,2,\ldots,K$), the number of replications B used in the simulation, and the multiset elements $S=\{(l_1^e,l_2^e,\ldots,l_m^e)\}_{e=1}^E$ for which the survival signature needs to be estimated. A counter $\phi'(l_1^e,l_2^e,\ldots,l_K^e)=0$ is initialized in Step 2 for each multiset element and used to count the number of replications in which the coverage remains at least α when exactly l_k^e functioning nodes remain in each region \mathcal{R}_k , $k=1,2,\ldots,K$. Steps 3–12 update the counts $\phi'(l_1^e,l_2^e,\ldots,l_K^e)$ while looping through the MC replications, and Step 13 outputs estimates the PSS Φ' by dividing

the counts $\phi'(l_1^e, l_2^e, \dots, l_K^e)$ by the number of MC replications. The following paragraph explains Steps 4–11, which comprise a single MC replication.

Algorithm 1 Monte Carlo algorithm for estimating the partial survival signature with respect to the collection of $(n_1, n_2, ..., n_K)$ -RGGs.

```
1: input: n_1, n_2, ..., n_K, B, S
 2: set \phi'(l_1^e, l_2^e, \dots, l_K^e) = 0, \forall e = 1, 2, \dots, E
 3: while L \leq B do
           Generate G by locating n_k nodes uniformly and independently within each subregion \mathcal{R}_k
                  for each k = 1, 2, \dots, K
           For every k = 1, 2, ..., K, simulate a random permutation \pi^k of the nodes in \mathcal{N}_k; \pi^k =
 5:
                  [i_1^k, i_2^k, \dots, i_{n_k}^k] where i_f^k is the fth-to-last node in \mathcal{N}_k to fail, \forall k = 1, 2, \dots, K
 6:
                if C[G \setminus \bigcup_{k=1}^{K} \{\pi^k(l_k^e + 1), \pi^k(l_k^e + 2), \dots, \pi^k(n_k)\}\} \ge \alpha then \phi'(l_1^e, l_2^e, \dots, l_K^e) = \phi'(l_1^e, l_2^e, \dots, l_K^e) + 1
 7:
 8:
 9:
           end for
10:
11: L = L + 1
12: end while
13: return \hat{\Phi}' = \{(1/B)\phi'(l_1^e, l_2^e, \dots, l_K^e)\}_{e=1}^E
```

At the beginning of each replication of Algorithm 1, Step 4 simulates a new (n_1, n_2, \ldots, n_K) -RGG \mathcal{G} with node sets \mathcal{N}_k defining the sensor nodes in \mathcal{R}_k , and Step 5 generates permutations π^k which specify the order in which sensor nodes in \mathcal{N}_k will fail. Let $\pi^k(l) \in \mathcal{N}_k$ $(l = 1, 2, \ldots, n_k, \forall k = 1, 2, \ldots, K)$ denote the l-th to last node to fail among the nodes in \mathcal{N}_k . Due to Assumption 1, the nodes within each class are equally likely to fail in any order; therefore, the n_k ! permutations of \mathcal{N}_k are generated for π^i with equal probability. Steps 6–10 comprise a loop in which the coverage of \mathcal{G} is evaluated (e.g., by running a breadth-first search from node 0) for all $e = 1, 2, \ldots, E$ with respect to the failure order defined by permutations π^k . If the coverage is at least α when for each $k = 1, 2, \ldots, K$ exactly l_k^e functioning sensor nodes remain in \mathcal{N}_k , the counter $\phi'(l_1^e, l_2^e, \ldots, l_K^e)$ is incremented.

Instance	r_1	r_2	r_3	r_4	r_5
K=2	0.1	0.7			
K = 3	0.1	0.4	0.7		
K = 4	0.1	0.25	0.45	0.7	
K = 5	0.1	0.25	0.45	0.65	0.7

Table 1: Parameter values specifying radius r_k for each subregion in each instance

7 Numerical Examples

In this section, we present numerical examples in which we (i) demonstrate the performance of the PSS estimate and (ii) apply optimization to identify TBDPs that are efficient with respect to cost and α -coverage reliability. The code for Algorithm 1 is implemented in Spyder using Python 3.2 and tested on a high performance computer supported by the Arkansas High Performance Computing Center.

In what follows, we examine instances involving $K \in \{2,3,4,5\}$ node classes. Throughout this section, we consider a circular region \mathcal{R} with a radius of r = 0.7 and a sink node located at coordinates (x,y) in the center of the region. The area allocated to each node class is adjusted based on the total number of classes. The region \mathcal{R} is divided into concentric subregions where r_k defines the outer radius of subregion \mathcal{R}_k , i.e.,

$$\mathcal{R}_k = \{(x_{n_k}, y_{n_k}) : r_{k-1} \le \sqrt{(x_{n_k} - x)^2 + (y_{n_k} - y)^2} \le r_k\} \quad k = 1, \dots, K.$$
(8)

The values of r_k for each k = 1, 2, ..., K in each instance $K \in \{2, 3, 4, 5\}$ are presented in Table 1. The communication radius d_1 and sensing range radius d_2 are set to 0.1. We located 81 target nodes across the network. The target nodes are arranged in a (9×9) grid within a (1×1) region, with the center of the grid coinciding with the location of the sink node. The distribution of target nodes ensures that it covers every subregion of the network.

Within each instance $K \in \{2, 3, 4, 5\}$, we assume sensor nodes in each class k = 1, 2, ..., K have Weibull lifetime with shape parameter $\beta_k = 1.5$ and scale parameter λ_k with values given in Table 2. Shape parameter values $\beta_k > 1$ are used to impose that sensor nodes become more likely to fail

Instance	λ_1	λ_2	λ_3	λ_4	λ_5
K=2	5	10			
K = 3	5	9	10		
K = 4	5	10	11	12	
K = 5	5	10	11	12	13

Table 2: Parameter values specifying Weibull time-to-failure distribution for each node class in each instance

as they age, e.g., to model the assumption of limited battery charge and/or degradation of battery capacity over time. The scale parameter (λ) value has proportional relation with the expected lifetime; thus, we assign $\lambda_1 < \lambda_2 < \cdots < \lambda_K$ to impose that sensor nodes closer to the sink (which have heavier traffic loads) have shorter expected lifetime. Figure 4 displays the reliability function associated with nodes in each class $k = 1, 2, \dots, 5$ in instance K = 5.

For each instance $K \in \{2,3,4,5\}$, we use Algorithm 1 with B=10,000 replications and $\alpha=0.8$ to estimate the PSS with respect to an $(\bar{n}_1,\bar{n}_2,\ldots,\bar{n}_K)$ -RGG, where \bar{n}_k is a given upper bound on the number of nodes in each class $k=1,2,\ldots,K$ (see Table 3). Let $\{\hat{\phi}(l_1^e,l_2^e,\ldots,l_K^e)\}_{e=1}^E$ and $\hat{\Phi}$ denote the estimated PSS survival signature elements of the $(\bar{n}_1,\bar{n}_2,\ldots,\bar{n}_K)$ -RGG, and let Φ denote the underlying (true) survival signature with elements $\phi(l_1,l_2,\ldots,l_K)$. Now consider the $(\bar{n}_1,\bar{n}_2,\ldots,\bar{n}_K)$ -RGG t>0 time units after node deployment, and suppose $n_k \leq \bar{n}_k$ functional nodes remain in each class $k=1,2,\ldots,K$ at this time. Because sensor nodes are randomly and independently located, the network at this time is an (n_1,n_2,\ldots,n_K) -RGG. Thus, letting $\bar{\phi}(l_1,l_2,\ldots,l_K)$ denote the survival signature elements of the (n_1,n_2,\ldots,n_K) -RGG, we have

$$\bar{\phi}(l_1, l_2, \dots, l_K) = \phi(l_1, l_2, \dots, l_K), \tag{9}$$

for all $l_k \in \{0, 1, ..., n_k\}$ and k = 1, 2, ..., K. Therefore, an estimate of the PSS for any $(n_1, n_2, ..., n_K)$ RGG with $n_k \leq \bar{n}_k$ for all k = 1, 2, ..., K can be extracted from $\hat{\Phi}$ by disregarding the elements $(l_1^e, l_2^e, ..., l_K^e)$, e = 1, ..., E, for which $l_k^e > n_k$ for some k = 1, 2, ..., K.

In what follows, we estimate the PSS using a variety of values of E and measure the impact on estimation error. The CPU time required for this step can be substantial, as shown in

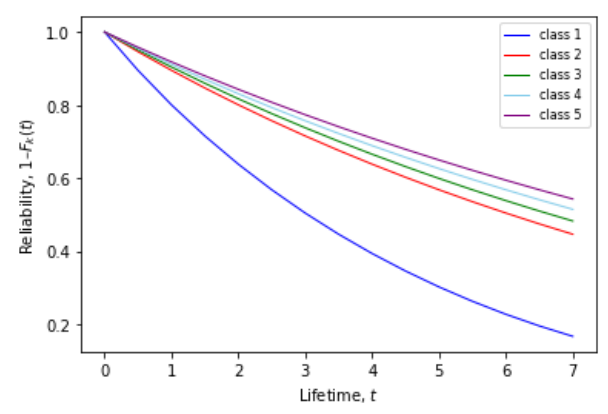


Figure 4: Reliability function $\bar{F}_k(t) = 1 - F_k(t)$ for nodes in each class k = 1, 2, ..., 5 in instance K = 5

Instance	\bar{n}_1	\bar{n}_2	\bar{n}_3	\bar{n}_4	\bar{n}_5
K=2	50	400			
K = 3	50	200	250		
K = 4	50	100	150	200	
K = 5	50	100	150	190	60

Table 3: Upper bounds on n_k in each instance

Table 4; however, following the discussion in the previous paragraph, this step need only be completed once. Thereafter, Equations (7) and (9) can used to estimate α -coverage reliability for any $(n_1, n_2, \dots, n_K; t')$ -TBDP with $n_k \leq \bar{n}_k$ for all $k = 1, 2, \dots, K$.

7.1 Evaluating α-Coverage Reliability Estimation Error

In this section, we provide numerical results to demonstrate the effectiveness of estimating α coverage reliability using the PSS and Equation (7). We want to assess the efficacy of the proposed PSS method with respect to estimation error and computation time; however, because it is

¹Due to run-time limitations on the (shared) hardware we utilized, this result was obtained by aggregating over multiple runs with only a subset of the elements.

Instance	Total PSS Elements, E	CPU Time (hours)
K=2	10,000	18.45
K = 3	30,000	64.29
K = 4	100,000	222.72
K = 5	100,000	343.35

Table 4: Time required to estimate the PSS elements for each node class in each instance¹

intractable to compute the true α-coverage reliability for large-scale networks, we compare the PSS estimate of α -coverage reliability against a Monte Carlo estimate of α -coverage reliability for which the error properties are known. The Monte Carlo method, hereafter referred to as Base MC, (i) simulates the state (functioning or failed) of each node $i \in \mathcal{N}_k$ in each class $k = 1, \dots, K$ according to probabilities $G_k(t'; t')$; and (ii) estimates α -coverage reliability as the proportion of replications yielding a coverage of at least α . Both the PSS and Base MC estimates of α -coverage reliability are produced for 200 TBDPs within each instance $K \in \{2,3,4,5\}$, and the differences between each pair of estimates are assessed relative to known properties of the Base MC error. Whereas Base MC must be repeated for each TBDP, the MC to estimate the PSS is run only once for each instance and the resulting PSS estimate is used in conjunction with Equations (7) and (9) to produce the α-coverage reliability estimate for each TBDP within the instance. The TBDPs are generated by selecting $n_k \in \{\underline{n}_k, \underline{n}_k + 1, \dots, \overline{n}_k\}$ at random (and with equally likely probability) for each $k \in \{1, 2, ..., K\}$, where values \bar{n}_k are specified in Table 3 and lower limits \underline{n}_k are chosen to ensure that the selection of TBDPs results in interesting α -coverage reliability values (e.g., not all close to zero). The value t' in each TBDP is selected randomly according to a continuous uniform distribution on the interval from 1 to 7.

To formalize our comparison, let X_q and Y_q respectively denote the PSS estimate and Base MC estimate of α -coverage reliability for a particular TBDP $q = [n_1, n_2, \ldots, n_K, t']$ for instance K, and suppose $p_q \equiv R(n_1, n_2, \ldots, n_K; t'; t')$ is the true (but unknown) α -coverage reliability for TBDP q. Assuming b MC replications are used to produce the estimate Y_q , the quantity bY_q is distributed binomial (b, p_q) and Y_q is therefore distributed approximately $N(p_q, p_q(1-p_q)/b)$, provided $bp_q > 5$ and $b(1-p_q) > 5$ [82, p. 344].

Now, supposing X_q has the same distribution as Y_q and is independent, then

$$W_{q} = \frac{X_{q} - Y_{q}}{\sqrt{\frac{2}{b} \left(\frac{X_{q} + Y_{q}}{2}\right) \left(1 - \frac{X_{q} + Y_{q}}{2}\right)}}$$
(10)

is distributed approximately N(0,1). This result forms the basis of the widely used large-sample

hypothesis test on the difference in population proportions [82, p. 415]. Thus, we compute W_q for TBDPs $1,2,\ldots,Q$ (where Q is the number of TBDPs) and compute \bar{W} as the sample mean and S^2 as the sample variance of $\{W_1,W_2,\ldots,W_Q\}$. Assuming the W_q -values are independent of each other and $\mathbb{E}[X_q]=p_q$, we should expect to see \bar{W} close to 0 and S^2 close to 1 in this case (i.e., if X_q has the same distribution as Y_q). Note that, to satisfy the required assumptions of the normal approximation to the binomial, we throw out TBDPs with $b(1-Y_q) \leq 5$ or $bY_q \leq 5$ prior to computing S^2 .

Although X_q and Y_q may not have the same distribution, we follow the above procedure (computing W_1, W_2, \dots, W_Q ; \bar{W} ; and S^2) to assess the accuracy and precision of the PSS estimate relative to Base MC. Specifically:

- To assess accuracy, we perform a t-test test (using \bar{W} and S^2) on the hypothesis that the mean W_q -value (i.e., as defined in Equation (10)) is equal to zero.
- To assess precision, we evaluate whether $S^2 < 1$, which would suggest that the PSS estimate is at least as precise as the Base MC estimate.

In assessing precision, we opted not to perform a statistical test on the variance of the W_q -value. As such, we note that observing $S^2 < 1$ in our results may not imply a statistically significant improvement in precision but rather that the PSS estimate of α -coverage reliability is more likely than not to be more precise than that of the Base MC.

Table 5 summarizes the experimental results for each instance $K \in \{2,3,4,5\}$ as we vary the number of elements E in the PSS. We report the number of elements in the PSS as a percentage of the number of elements in Φ (see column "Density"); \bar{W} and S^2 (both defined in the previous paragraph); and also the average CPU time per TBDP (see column "CPU Time") required to (re)evaluate the α -coverage reliability estimate given that the PSS estimate has already been obtained. In addition, we summarize the P-value resulting from the t-test. Here, note that a small P-value (e.g., P < 0.05 or P < 0.1), suggests that the mean W_q -value is not close to 0, and a larger P-value indicates it is more plausible for the mean W_q -value to be close to 0.

Instance	PSS Elements, E	Density	CPU Time (sec/TBDP)	$ar{W}$	S^2	P-Value
K=2	5000	25%	1.06	0.11	0.61	0.15
	10000	50%	1.70	0.08	0.61	0.27
	20000	100%	3.05	0.04	0.54	0.64
K=3	10000	0.4%	2.72	-0.14	1.23	0.11
	20000	0.8%	4.89	0.05	1.17	0.58
	30000	0.12%	7.05	0.09	0.76	0.19
K=4	25000	0.0167%	8.20	0.02	2.02	0.84
	50000	0.0334%	16.38	-0.08	1.40	0.41
	100000	0.0667%	31.29	-0.01	0.98	0.90
K=5	25000	0.0012%	11.43	0.18	10.08	0.46
	50000	0.00234%	21.14	-0.01	5.42	0.58
	100000	0.0012%	40.63	-0.08	2.82	0.54

Table 5: Experimental Results Summary

We first examine the results of Table 5 with regard to the accuracy of the PSS estimate. From Table 5, we notice that for \bar{W} tends to be close to 0, especially as the PSS density is increased. Additionally, the large P-values (especially with regard to larger values of E) suggest that the PSS estimate of α -coverage reliability has little bias, or perhaps none. Because these P-values require an assumption of normality, we present probability plots in Appendix C to demonstrate that the normal distribution appears reasonable for the W_q -values.

Toward assessing the precision of the PSS estimate, we observe that S^2 decreases for instances $K \in \{2,3,4,5\}$ as the number of elements in the PSS increases. This is an expected result because Equation (6) is an exact characterization of α -coverage reliability when all elements are used in the PSS. Because adding PSS elements increases CPU time, we are interested in identifying values of E in which $S^2 < 1$ and the CPU time per TBDP evaluation is less for PSS than Base MC. We are able to achieve $S^2 < 1$ in 1.059 seconds/TBDP for K = 2 (using E = 5,000), 7.048 seconds/TBDP for K = 3 (using E = 30,000), and 31.29 seconds/TBDP for K = 4 (using E = 100,000), respectively. On the other hand, the corresponding running times for Base MC were substantially greater at 109.59, 142.57, and 114.87 seconds. Although the PSS yields a favorable alternative to Base MC for $K \in \{2,3,4\}$, it does not appear to be preferable for K = 5. Although it may be possible to decrease S^2 for K = 5 by further increasing E, doing so would also increasing the running time. Because the CPU time per TBDP with K = 5 and E = 100,000 is already of a similar magnitude

as the Base MC time, the current approach does not appear to be advantageous for K = 5.

In what follows, we examine an optimization problem in which we seek to identify TBDPs that are efficient with respect to cost and α -coverage reliability. We solve this optimization problem using a metaheuristic that requires repeated evaluation of α -coverage reliability. From the above discussions, the PSS estimate can be evaluated faster (and without sacrificing accuracy or precision) in such scenarios where we need to evaluate the α -coverage reliability of many TBDPs. On the other hand, Base MC does not admit an efficient reevaluation of α -coverage reliability; thus, this method is prohibitive for optimization in the case of large-scale systems.

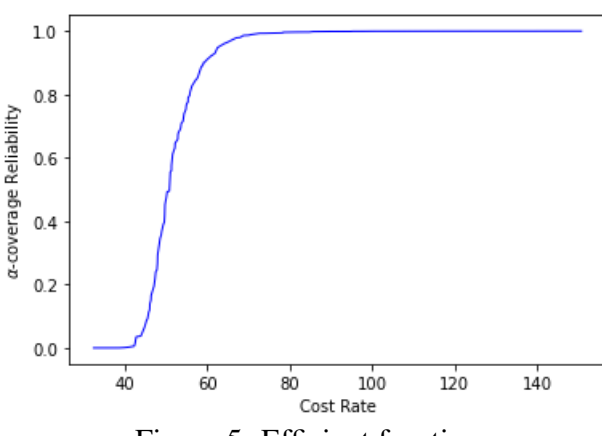
7.2 Identifying Efficient Redeployment Policies

Having demonstrated the effectiveness of estimating α -coverage reliability using the PSS and Equation (7), we now seek to identify TBDPs that are efficient with respect to cost and α -coverage reliability. To this end, let c_f denote a fixed cost incurred each time nodes are deployed and let c_v denote a variable cost per node deployed. We consider the multi-objective optimization model

$$\max_{n_1, n_2, \dots, n_K; t'} \left\{ \hat{R}(n_1, n_2, \dots, n_K; t'; t'), -C(n_1, n_2, \dots, n_K; t') \right\}, \tag{11}$$

where $C(n_1, n_2, ..., n_K; t') = (c_f + \sum_{k=1}^K n_k c_v G_k(t'; t'))/t'$ represents the cost rate of the TBDP $(n_1, n_2, ..., n_K; t')$, following a similar concept introduced in [66]. For each instance $K \in \{2, 3, 4, 5\}$, we set $c_f = 100$ and $c_v = 1$ for all node classes.

To identify near-efficient TBDPs for Model (11), we apply non-dominated sorting genetic algorithm II (NSGA-II) [83] using an adaptation of the source code developed by [84], wherein the α -coverage reliability objective is evaluated through Equations (7) and (9) using the PSS estimate $\hat{\Phi}$. Below, we present the optimization results for instance K = 4. For our tests, we constrain $n_1 \in \{10,11,\ldots,50\}, n_2 \in \{50,51,\ldots,100\}, n_3 \in \{75,76,\ldots,150\}, \text{ and } n_4 \in \{100,101,\ldots,200\}$ and restrict the redeployment interval t' to be between 1 and 7. For the NSGA-II experiments, we use a crossover probability of 0.6 and mutation probability of 0.2. The distribution index for



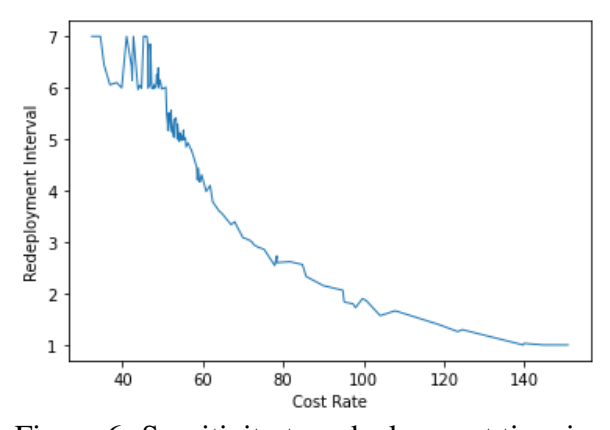


Figure 5: Efficient frontier

Figure 6: Sensitivity to redeployment time interval

crossover and mutation parameters are set to 2 and 10, respectively. (Note: The distribution index for crossover controls the *crowding distance*, i.e., a measure of the concentration of solutions within specific regions of the Pareto front. The distribution index for mutation controls the mutation applied to individual genes, where the mutation is responsible for making a small change to an individual's decision variables to explore the solution space.) We use a population size of 100 and 20 generations, requiring approximately 47.5 hours of CPU time in addition to the time required produce the PSS estimate $\hat{\Phi}$. Appendix B provides convergence analysis to demonstrate that additional generations are unlikely to yield substantial gains in solution quality.

We summarize the results through a series of plots that depict the relation between objective functions the decision variables. Figure 5 presents a summary of α -coverage reliability versus cost rate for TBDPs on the (near) efficient frontier. To examine the structure of the obtained near-efficient frontier, we plot each near-efficient TBDP's variable values versus its cost-rate (i.e., the value plotted on the horizontal axis in Figure 5). Figure 6 shows the relation between cost and redeployment interval, t'. From Figure 5 and 6, it is observed that as the redeployment interval decreases, α -coverage reliability improves; however, the cost of redeployment is increasing. It is possible to achieve over 99% α -coverage reliability with t' < 3, but marginal gains beyond this point require a substantial increase in cost rate.

Figures 7–10 depict the relationship between cost rate and n_k , k = 1,2,3,4. Among the near-efficient TBDPs with cost rate less than 85, Figures 7–10 show a positive relationship between

cost rate and the number of nodes in each region where both n_3 and n_4 reach their maximum limit. This is an expected result: If we are willing to spend more overall, we should expect to allocate more resources to each subregion. This pattern changes when considering near-efficient TBDPs with cost rate greater than 85. Presumably, this is because all such near-efficient TBDPs have α -coverage reliability greater than 0.9968. As such, we speculate that there are a large number of other TBDPs that achieve a similar cost and α -coverage reliability. In combination with the possibility of error in the PSS estimate, this leads to variability in the TBDPs identified as near-efficient.

Figure 11 and Figures 12-15 provide an insight into how optimal policy changes with respect to the changes in the shape (β) and scale (λ) parameter. From Figure 11 and Figure 12, we notice that the results do not change substantially in response to small changes in β and λ_1 . The insensitivity to change in λ_1 is expected as the redeployment decision are accounting for the heavier traffic load the fact that these nodes are used to relay. For λ_2 , λ_3 , and λ_4 , either a 20% decrease or 25% increase substantially changes the results, where greater α-coverage reliability can be achieved for the same cost when the λ -values are greater. However, the sensitivity to λ_1 , λ_2 , and λ_3 become less pronounced when the cost rate is greater than 80, which is expected as higher cost corresponds a shorter redeployment interval. We conducted an additional sensitivity analysis to examine the degree to which misspecifying λ or β may result in sub-optimal solutions. Specifically, we evaluate the near-efficient policies for $\beta = 1.3$ and $\beta = 1.7$ with respect to the cost and α -coverage reliability for $\beta = 1.5$. As illustrated in Figure 16, the resulting efficient frontier plots closely resemble those for the $\beta = 1.5$ case, so the near-efficient TBDPs are robust to such changes in β . Likewise, we evaluated the near-efficient policies with respect to the base λ -values (see Table 2) for the cost and α -coverage reliability when all λ -values are decreased by 20% or increased by 25%. As shown in Figure 17, the near-efficient TBDPs are also robust against changes in λ .

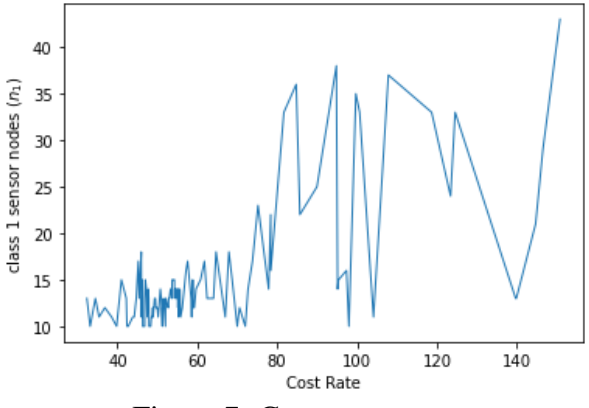


Figure 7: Cost rate vs. n_1

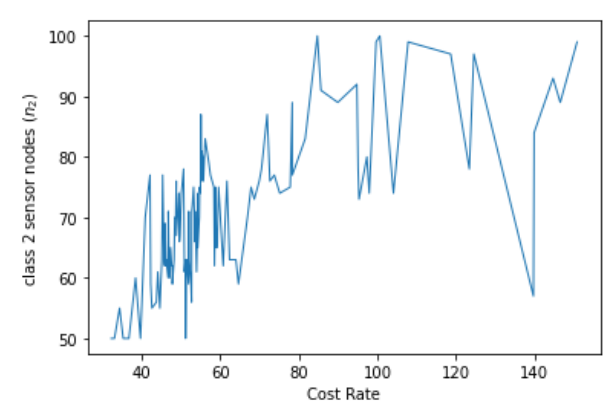


Figure 8: Cost rate vs n_2

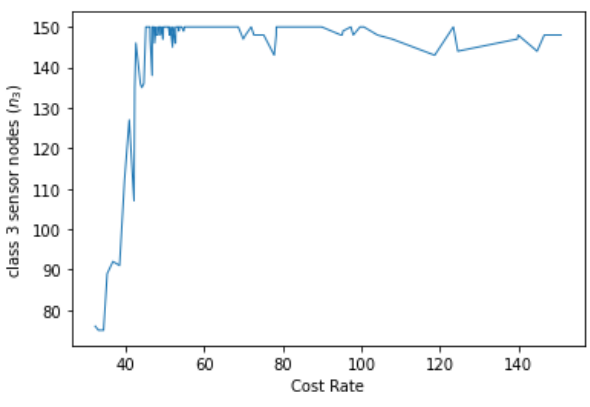


Figure 9: Cost rate vs. n_3

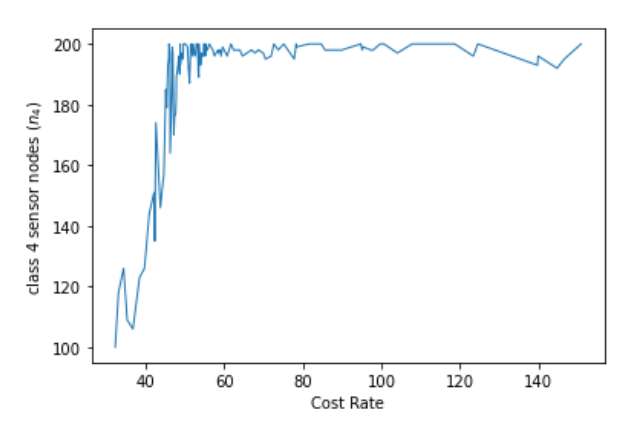


Figure 10: Cost rate vs. n_4

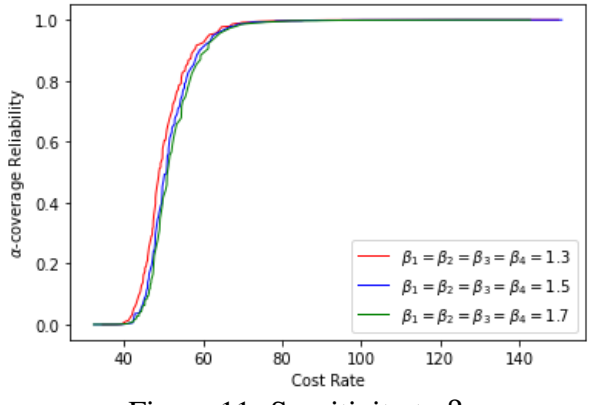


Figure 11: Sensitivity to β

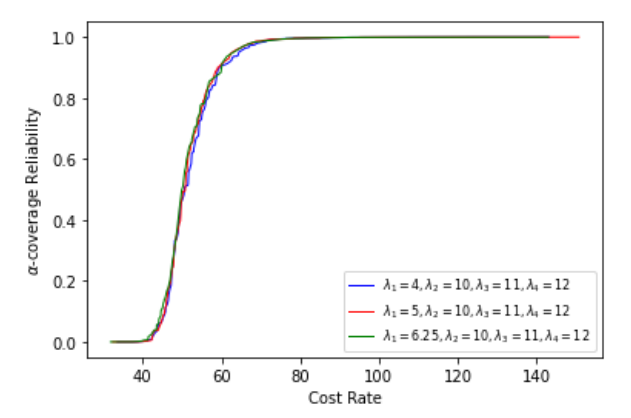
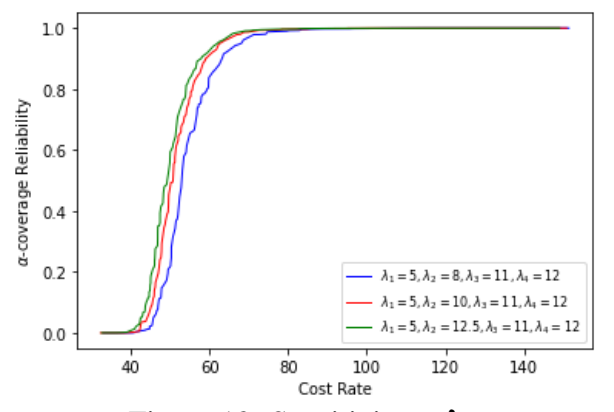


Figure 12: Sensitivity to λ_1



1.0

0.8

0.8

0.4

0.0

0.2

0.0

0.0

0.1

0.0

0.0

0.1

0.0

0.0

0.0

0.0

0.0

0.0

0.0

0.0

0.0

0.0

0.0

0.0

0.0

0.0

0.0

0.0

0.0

0.0

0.0

0.0

0.0

0.0

0.0

0.0

0.0

0.0

0.0

0.0

0.0

0.0

0.0

0.0

0.0

0.0

0.0

0.0

0.0

0.0

0.0

0.0

0.0

0.0

0.0

0.0

0.0

0.0

0.0

0.0

0.0

0.0

0.0

0.0

0.0

0.0

0.0

0.0

0.0

0.0

0.0

0.0

0.0

0.0

0.0

0.0

0.0

0.0

0.0

0.0

0.0

0.0

0.0

0.0

0.0

0.0

0.0

0.0

0.0

0.0

0.0

0.0

0.0

0.0

0.0

0.0

0.0

0.0

0.0

0.0

0.0

0.0

0.0

0.0

0.0

0.0

0.0

0.0

0.0

0.0

0.0

0.0

0.0

0.0

0.0

0.0

0.0

0.0

0.0

0.0

0.0

0.0

0.0

0.0

0.0

0.0

0.0

0.0

0.0

0.0

0.0

0.0

0.0

0.0

0.0

0.0

0.0

0.0

0.0

0.0

0.0

0.0

0.0

0.0

0.0

0.0

0.0

0.0

0.0

0.0

0.0

0.0

0.0

0.0

0.0

0.0

0.0

0.0

0.0

0.0

0.0

0.0

0.0

0.0

0.0

0.0

0.0

0.0

0.0

0.0

0.0

0.0

0.0

0.0

0.0

0.0

0.0

0.0

0.0

0.0

0.0

0.0

0.0

0.0

0.0

0.0

0.0

0.0

0.0

0.0

0.0

0.0

0.0

0.0

0.0

0.0

0.0

0.0

0.0

0.0

0.0

0.0

0.0

0.0

0.0

0.0

0.0

0.0

0.0

0.0

0.0

0.0

0.0

0.0

0.0

0.0

0.0

0.0

0.0

0.0

0.0

0.0

0.0

0.0

0.0

0.0

0.0

0.0

0.0

0.0

0.0

0.0

0.0

0.0

0.0

0.0

0.0

0.0

0.0

0.0

0.0

0.0

0.0

0.0

0.0

0.0

0.0

0.0

0.0

0.0

0.0

0.0

0.0

0.0

0.0

0.0

0.0

0.0

0.0

0.0

0.0

0.0

0.0

0.0

0.0

0.0

0.0

0.0

0.0

0.0

0.0

0.0

0.0

0.0

0.0

0.0

0.0

0.0

0.0

0.0

0.0

0.0

0.0

0.0

0.0

0.0

0.0

0.0

0.0

0.0

0.0

0.0

0.0

0.0

0.0

0.0

0.0

0.0

0.0

0.0

0.0

0.0

0.0

0.0

0.0

0.0

0.0

0.0

0.0

0.0

0.0

0.0

0.0

0.0

0.0

0.0

0.0

0.0

0.0

0.0

0.0

0.0

0.0

0.0

0.0

0.0

0.0

0.0

0.0

0.0

0.0

0.0

0.0

0.0

0.0

0.0

0.0

0.0

0.0

0.0

0.0

0.0

0.0

0.0

0.0

0.0

0.0

0.0

0.0

0.0

0.0

0.0

0.0

0.0

0.0

0.0

0.0

0.0

0.0

0.0

0.0

0.0

0.0

0.0

0.0

0.0

0.0

0.0

0.0

0.0

0.0

0.0

0.0

0.0

0.0

0.0

0.0

0.0

0.0

0.0

0.0

0.0

0.0

0.0

0.0

0.0

0.0

0.0

0.0

0.0

0.0

0.0

0.0

0.0

0.0

0.0

0.0

0.0

0.0

0.0

0.0

0.0

0.0

0.0

0.0

0.0

0.0

0.0

0.0

Figure 13: Sensitivity to λ_2

Figure 14: Sensitivity to λ_3

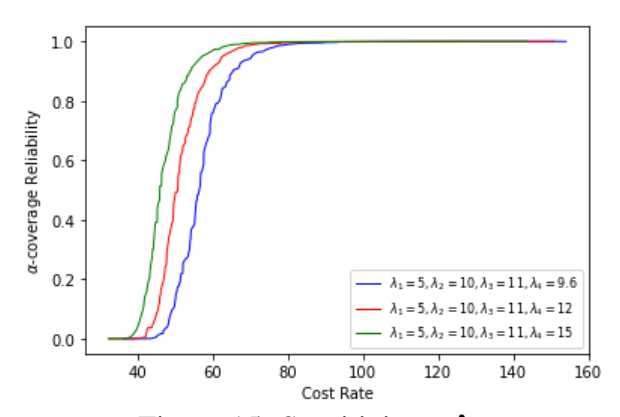


Figure 15: Sensitivity to λ_4

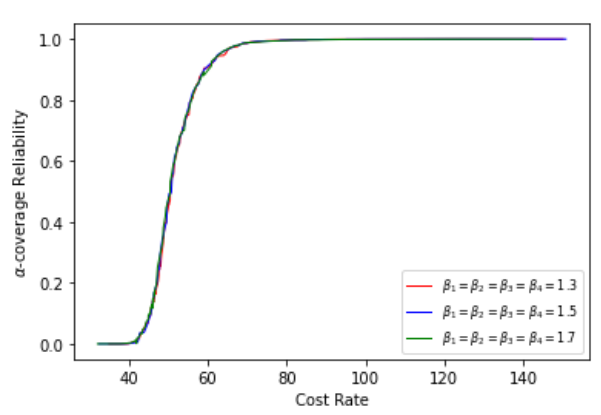


Figure 16: Reevaluation of near-efficient TB-DPs (for $\beta=1.3$ and $\beta=1.7$) with respect to cost and α -coverage reliability for $\beta=1.5$

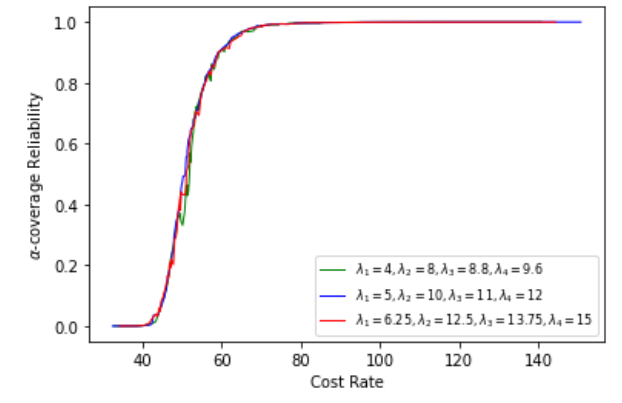


Figure 17: Reevaluation of near-efficient TB-DPs (for λ decreased by 20% or increased by 25%) with respect to cost and α -coverage reliability for original λ -values

7.3 Summary of Results

To summarize the results section, we first validated the efficiency of the proposed PSS method by comparing it with Base MC (i.e., estimating α -coverage reliability directly by MC) in terms of estimation error and computation time per TBDP on numerical examples. For $K \leq 4$ (but not K = 5), the results suggest that the proposed method achieves estimation error that is comparable to Base MC in substantially less computational time. This reduction in computational time is due to the PSS method's ability to reuse computations in evaluating the α -coverage reliability of different TBDPs for the same problem instance.

Later, we applied NSGA-II to identify TBDPs that are efficient with respect to redeployment cost and α -coverage reliability. This analysis characterizes the tradeoff between these two metrics while highlighting how the (near-efficient) TBDP changes for different cost thresholds. These observations are crucial for decision-makers, as they provide valuable insights for both designing the WSN and planning node redeployment in consideration of the impacts on cost and α -coverage reliability.

8 Conclusion

In this work, we have considered the problem of redeploying unreliable sensor nodes into a multi-hop WSN with the objective of maximizing network reliability and minimizing overall deployment costs. We have established a survival signature characterization of the WSN's α -coverage reliability under a given time-based node deployment policy and multiple classes of unreliable nodes. Our work extends the related literature by allowing nodes' time-to-failure distribution to be dependent on positioning in the network, whereas previous research assumes i.i.d. node failures. The paper also contributes a method for estimating α -coverage reliability based on estimating only a portion of the elements in the survival signature (i.e., the PSS). Using numerical examples, we demonstrate that the resulting estimate of α -coverage reliability outperforms a straightforward Monte Carlo estimate (in terms of accuracy, precision, and CPU time) as long as there are not too many

node classes (e.g., for $K \le 4$ node classes in our instances). Furthermore, because the PSS need only be estimated once for a given instance, the resulting estimate of α -coverage reliability can be re-evaluated quickly. We have leveraged this result by employing NSGA-II to identify time-based node deployment policies that are near-efficient with respect to cost and α -coverage reliability, and we have discussed structural relationships among near-efficient node deployment policies corresponding to different cost thresholds.

Although the survival signature has received substantial recent attention in the literature, the use of the survival signature to estimate system reliability has usually been limited to systems that are smaller in scale than the 500-plus node instances examined in our study; therefore, the idea to use only a PSS may be attractive for estimating reliability in other large-scale, complex systems.

Our work opens several avenues for follow-on research. Whereas our work uses an unsophisticated approach (i.e., equally likely with replacement) to sampling survival signature elements for inclusion in the PSS, more sophisticated sampling approaches may yield additional improvements to the accuracy and precision of the PSS estimate of α -coverage reliability. Note, however, that the equally likely assumption is important in the sense of Equation (9): Because the sampled PSS elements $(l_1^e, l_2^e, \dots, l_K^e)$ are equally likely among the outcomes $\{0, 1, \dots, \bar{n}_1\} \times \{0, 1, \dots, \bar{n}_2\} \times \dots \times \{0, 1, \dots, \bar{n}_K\}$, when disregarding the sampled elements $(l_1^e, l_2^e, \dots, l_K^e)$ with $l_k^e > n_k$ for some $k = 1, 2, \dots, K$, the remaining elements can be considered as equally likely among the outcomes $\{0, 1, \dots, n_1\} \times \{0, 1, \dots, n_2\} \times \dots \times \{0, 1, \dots, n_K\}$.

Additional follow-on research may seek to enhance Algorithm 1 for estimating the elements of the PSS. For example, we note that Step 7 requires evaluating the coverage of the network $\mathcal{G}(e) \equiv \mathcal{G} \setminus \bigcup_{k=1}^K \{\pi^k(l_k^e+1), \pi^k(l_k^e+2), \dots, \pi^k(n_k) \text{ for each PSS element } e=1,2,\dots,E.$ However, for any two elements $e, e' \in \{1,2,\dots,E\}$ with $l_k^e \leq l_k^{e'}$ for each $k=1,2\dots,K$, observe that $\mathcal{G}(e')$ can be obtained from $\mathcal{G}(e)$ by adding some nodes and their adjacent arcs. Therefore, rather than evaluating $C[\mathcal{G}(e')]$ by executing a (new) breadth-first search, it is possible to initialize this search using the output of the breadth-first search conducted to evaluate $C[\mathcal{G}(e)]$. Based upon further extensions of this idea, Lopes da Silva and Sullivan [75] (i) show that MC simulation of the (com-

plete) survival signature for a two-terminal network entails solving a multi-objective maximum capacity path (MOMCP) problem in each replication (ii) and demonstrate that, for the case of two node classes, solving the MOMCP using a specialized algorithm substantially improves the rate at which MC replications can be completed. Because the problem considered in our paper is substantially more general than [75] (e.g., estimating α -coverage reliability instead of two-terminal reliability, including K > 2 node classes instead of only two node classes, and evaluating only a portion of the survival signature elements instead of all elements), it is unclear whether such ideas can also lead to enhancements in Algorithm 1.

References

- [1] M. Younis, I. F. Senturk, K. Akkaya, S. Lee, and F. Senel, "Topology management techniques for tolerating node failures in wireless sensor networks: a survey," *Computer Networks*, vol. 58, pp. 254–283, 2014.
- [2] G. Wenqi and W. M. Healy, "Power supply issues in battery reliant wireless sensor networks: a review," *International Journal of Intelligent Control and Systems*, vol. 19, no. 1, pp. 15–23, 2014.
- [3] S. Yasin, T. Ali, U. Draz, A. Shaf, and M. Ayaz, "A parametric performance evaluation of batteries in wireless sensor networks," in *Recent Trends and Advances in Wireless and IoT-Enabled Networks*. Springer, 2019, pp. 187–196.
- [4] D. Wang, B. Xie, and D. P. Agrawal, "Coverage and lifetime optimization of wireless sensor networks with gaussian distribution," *IEEE Transactions on Mobile Computing*, vol. 7, no. 12, pp. 1444–1458, 2008.
- [5] I. B. Gertsbakh and Y. Shpungin, *Models of network reliability: analysis, combinatorics, and Monte Carlo*. CRC press, 2016.
- [6] J. Lian, K. Naik, and G. B. Agnew, "Data capacity improvement of wireless sensor networks using non-uniform sensor distribution," *International Journal of Distributed Sensor Networks*, vol. 2, no. 2, pp. 121–145, 2006.
- [7] C.-Y. Chang and H.-R. Chang, "Energy-aware node placement, topology control and MAC scheduling for wireless sensor networks," *Computer Networks*, vol. 52, no. 11, pp. 2189–2204, 2008.
- [8] V. Kumar, S. B. Dhok, R. Tripathi, and S. Tiwari, "Cluster size optimization in gaussian distributed wireless sensor networks," *International Journal of Engineering and Technology* (*IJET*), vol. 6, no. 3, pp. 1581–1592, 2014.
- [9] Y. Liu, H. Ngan, and L. M. Ni, "Power-aware node deployment in wireless sensor networks," *International Journal of Distributed Sensor Networks*, vol. 3, no. 2, pp. 225–241, 2007.
- [10] X. Wu, G. Chen, and S. K. Das, "Avoiding energy holes in wireless sensor networks with nonuniform node distribution," *IEEE Transactions on Parallel and Distributed Systems*, vol. 19, no. 5, pp. 710–720, 2008.
- [11] A. Demertzis and K. Oikonomou, "Avoiding energy holes in wireless sensor networks with non-uniform energy distribution," in *IISA 2014, The 5th International Conference on Information, Intelligence, Systems and Applications.* IEEE, 2014, pp. 138–143.
- [12] X. Liu, "Node deployment based on extra path creation for wireless sensor networks on mountain roads," *IEEE Communications Letters*, vol. 21, no. 11, pp. 2376–2379, 2017.

- [13] S. H. Singh, K. R. Verma, and P. Rajpoot, "Partition based strategic node placement and efficient communication method for WSN," in 2018 3rd IEEE International Conference on Recent Trends in Electronics, Information & Communication Technology (RTEICT). IEEE, 2018, pp. 1807–1812.
- [14] C. Ma, W. Liang, M. Zheng, and H. Sharif, "A connectivity-aware approximation algorithm for relay node placement in wireless sensor networks," *IEEE Sensors Journal*, vol. 16, no. 2, pp. 515–528, 2015.
- [15] B. O. Ayinde and H. A. Hashim, "Energy-efficient deployment of relay nodes in wireless sensor networks using evolutionary techniques," *International Journal of Wireless Information Networks*, vol. 25, pp. 157–172, 2018.
- [16] J. Xie, B. Zhang, and C. Zhang, "A novel relay node placement and energy efficient routing method for heterogeneous wireless sensor networks," *IEEE Access*, vol. 8, pp. 202439–202444, 2020.
- [17] M. A. Benatia, M. Sahnoun, D. Baudry, A. Louis, A. El-Hami, and B. Mazari, "Multi-objective WSN deployment using genetic algorithms under cost, coverage, and connectivity constraints," *Wireless Personal Communications*, vol. 94, no. 4, pp. 2739–2768, 2017.
- [18] S. Mini, S. K. Udgata, and S. L. Sabat, "Sensor deployment and scheduling for target coverage problem in wireless sensor networks," *IEEE Sensors Journal*, vol. 14, no. 3, pp. 636–644, 2013.
- [19] J. Yu, S. Wan, X. Cheng, and D. Yu, "Coverage contribution area based *k*-coverage for wireless sensor networks," *IEEE Transactions on Vehicular Technology*, vol. 66, no. 9, pp. 8510–8523, 2017.
- [20] S. Misra, S. D. Hong, G. Xue, and J. Tang, "Constrained relay node placement in wireless sensor networks to meet connectivity and survivability requirements," in *IEEE INFOCOM 2008-The 27th Conference on Computer Communications*. IEEE, 2008, pp. 281–285.
- [21] H. M. Almasaeid and A. E. Kamal, "On the minimum *k*-connectivity repair in wireless sensor networks," in *2009 IEEE International Conference on Communications*. IEEE, 2009, pp. 1–5.
- [22] S. Sengupta, S. Das, M. Nasir, and B. K. Panigrahi, "Multi-objective node deployment in WSNs: In search of an optimal trade-off among coverage, lifetime, energy consumption, and connectivity," *Engineering Applications of Artificial Intelligence*, vol. 26, no. 1, pp. 405–416, 2013.
- [23] O. Ben Amor, Z. Chelly Dagdia, S. Bechikh, and L. Ben Said, "Many-objective optimization of wireless sensor network deployment," *Evolutionary Intelligence*, pp. 1–17, 2022.
- [24] K. Magklara, D. Zorbas, and T. Razafindralambo, "Node discovery and replacement using mobile robot," in *International Conference on Ad Hoc Networks*. Springer, 2012, pp. 59–71.

- [25] B. Tong, G. Wang, W. Zhang, and C. Wang, "Node reclamation and replacement for long-lived sensor networks," *IEEE Transactions on Parallel and Distributed Systems*, vol. 22, no. 9, pp. 1550–1563, 2011.
- [26] S. Parikh, V. M. Vokkarane, L. Xing, and D. Kasilingam, "Node-replacement policies to maintain threshold-coverage in wireless sensor networks," in 2007 16th International Conference on Computer Communications and Networks. IEEE, 2007, pp. 760–765.
- [27] A. G. Ramonet and T. Noguchi, "Node replacement method for disaster resilient wireless sensor networks," in 2020 10th Annual Computing and Communication Workshop and Conference (CCWC). IEEE, 2020, pp. 0789–0795.
- [28] A. K. Mohapatra, N. Gautam, and R. L. Gibson, "Combined routing and node replacement in energy-efficient underwater sensor networks for seismic monitoring," *IEEE Journal of Oceanic Engineering*, vol. 38, no. 1, pp. 80–90, 2012.
- [29] S.-J. Park and R. Sivakumar, "Sink-to-sensors reliability in sensor networks," *ACM SIGMO-BILE Mobile Computing and Communications Review*, vol. 7, no. 3, pp. 27–28, 2003.
- [30] Y. Sankarasubramaniam, Ö. B. Akan, and I. F. Akyildiz, "ESRT: event-to-sink reliable transport in wireless sensor networks," in *Proceedings of the 4th ACM International Symposium on Mobile ad Hoc Networking & Computing*, 2003, pp. 177–188.
- [31] H. M. AboElFotoh, S. S. Iyengar, and K. Chakrabarty, "Computing reliability and message delay for cooperative wireless distributed sensor networks subject to random failures," *IEEE transactions on reliability*, vol. 54, no. 1, pp. 145–155, 2005.
- [32] H. M. AboElFotoh, E. S. ElMallah, and H. S. Hassanein, "On the reliability of wireless sensor networks," in *2006 IEEE International Conference on Communications*, vol. 8. IEEE, 2006, pp. 3455–3460.
- [33] Y. Xiao, X. Li, Y. Li, and S. Chen, "Evaluate reliability of wireless sensor networks with OBDD," in 2009 IEEE International Conference on Communications. IEEE, 2009, pp. 1–5.
- [34] Y.-F. Xiao, S.-Z. Chen, L. Xin, and Y.-H. Li, "Reliability evaluation of wireless sensor networks using an enhanced OBDD algorithm," *The Journal of China Universities of Posts and Telecommunications*, vol. 16, no. 5, pp. 62–70, 2009.
- [35] A. Shrestha, L. Xing, and H. Liu, "Modeling and evaluating the reliability of wireless sensor networks," in 2007 Annual Reliability and Maintainability Symposium. IEEE, 2007, pp. 186–191.
- [36] J. L. Cook and J. E. Ramirez-Marquez, "Two-terminal reliability analyses for a mobile ad hoc wireless network," *Reliability Engineering & System Safety*, vol. 92, no. 6, pp. 821–829, 2007.
- [37] B. Chen, A. Phillips, and T. I. Matis, "Two-terminal reliability of a mobile ad hoc network under the asymptotic spatial distribution of the random waypoint model," *Reliability Engineering & System Safety*, vol. 106, pp. 72–79, 2012.

- [38] G. Egeland and P. E. Engelstad, "The availability and reliability of wireless multi-hop networks with stochastic link failures," *IEEE Journal on Selected Areas in Communications*, vol. 27, no. 7, pp. 1132–1146, 2009.
- [39] M. M. Singh and J. K. Mandal, "Reliability analysis of mobile ad hoc network," in 2015 International Conference on Computational Intelligence and Communication Networks (CICN). IEEE, 2015, pp. 161–164.
- [40] J. E. Ramirez-Marquez and C. M. Rocco, "All-terminal network reliability optimization via probabilistic solution discovery," *Reliability Engineering & System Safety*, vol. 93, no. 11, pp. 1689–1697, 2008.
- [41] J.-H. Park, "All-terminal reliability analysis of wireless networks of redundant radio modules," *IEEE Internet of Things Journal*, vol. 3, no. 2, pp. 219–230, 2015.
- [42] Y. Xiao, S. Chen, X. Li, and Y. Li, "An enhanced factoring algorithm for reliability evaluation of wireless sensor networks," in 2008 The 9th International Conference for Young Computer Scientists. IEEE, 2008, pp. 2175–2179.
- [43] C. Chowdhury, N. Aslam, G. Ahmed, S. Chattapadhyay, S. Neogy, and L. Zhang, "Novel algorithms for reliability evaluation of remotely deployed wireless sensor networks," *Wireless Personal Communications*, vol. 98, no. 1, pp. 1331–1360, 2018.
- [44] G. Yang, T. Liang, X. He, and N. Xiong, "Global and local reliability-based routing protocol for wireless sensor networks," *IEEE Internet of Things Journal*, vol. 6, no. 2, pp. 3620–3632, 2018.
- [45] S. Chakraborty, N. K. Goyal, S. Mahapatra, and S. Soh, "Minimal path-based reliability model for wireless sensor networks with multistate nodes," *IEEE Transactions on Reliability*, vol. 69, no. 1, pp. 382–400, 2019.
- [46] H. Luo, H. Tao, H. Ma, and S. K. Das, "Data fusion with desired reliability in wireless sensor networks," *IEEE Transactions on Parallel and Distributed Systems*, vol. 22, no. 3, pp. 501–513, 2010.
- [47] J. Zhang, P. Hu, F. Xie, J. Long, and A. He, "An energy efficient and reliable in-network data aggregation scheme for WSN," *IEEE Access*, vol. 6, pp. 71857–71870, 2018.
- [48] A. E. Zonouz, L. Xing, V. M. Vokkarane, and Y. Sun, "k-coverage reliability evaluation for wireless sensor networks," in *Proc. 18th ISSAT Int. Conf. Rel. Qual. Des.*, 2012.
- [49] Y.-L. Jin, H.-J. Lin, Z.-M. Zhang, Z. Zhang, and X.-Y. Zhang, "Estimating the reliability and lifetime of wireless sensor network," in 2008 4th International Conference on Wireless Communications, Networking and Mobile Computing. IEEE, 2008, pp. 1–4.
- [50] Q. Yang and Y. Chen, "Monte Carlo methods for reliability evaluation of linear sensor systems," *IEEE Transactions on Reliability*, vol. 60, no. 1, pp. 305–314, 2011.

- [51] S. Xiang and J. Yang, "Reliability evaluation and reliability-based optimal design for wireless sensor networks," *IEEE Systems Journal*, vol. 14, no. 2, pp. 1752–1763, 2019.
- [52] S. Chakraborty, N. K. Goyal, and S. Soh, "On area coverage reliability of mobile wireless sensor networks with multistate nodes," *IEEE Sensors Journal*, vol. 20, no. 9, pp. 4992–5003, 2020.
- [53] K. Khoshraftar and B. Heidari, "A hybrid method based on clustering to improve the reliability of the wireless sensor networks," *Wireless Personal Communications*, vol. 113, no. 2, pp. 1029–1049, 2020.
- [54] L. Cao, Y. Yue, Y. Cai, and Y. Zhang, "A novel coverage optimization strategy for heterogeneous wireless sensor networks based on connectivity and reliability," *IEEE Access*, vol. 9, pp. 18424–18442, 2021.
- [55] A. Banerjee, M. Gavrilas, O. Ivanov, and S. Chattopadhyay, "Reliability improvement and the importance of power consumption optimization in wireless sensor networks," in 2015 9th International Symposium on Advanced Topics in Electrical Engineering (ATEE). IEEE, 2015, pp. 735–740.
- [56] D. S. Deif and Y. Gadallah, "An ant colony optimization approach for the deployment of reliable wireless sensor networks," *IEEE Access*, vol. 5, pp. 10744–10756, 2017.
- [57] M. Hashimoto, N. Wakamiya, M. Murata, Y. Kawamoto, and K. Fukui, "End-to-end reliability-and delay-aware scheduling with slot sharing for wireless sensor networks," in 2016 8th International Conference on Communication Systems and Networks (COMSNETS). IEEE, 2016, pp. 1–8.
- [58] C. Zhang, J. Yang, and N. Wang, "Timely reliability modeling and evaluation of wireless sensor networks with adaptive n-policy sleep scheduling," *Reliability Engineering & System Safety*, vol. 235, p. 109270, 2023.
- [59] —, "An active queue management for wireless sensor networks with priority scheduling strategy," *Journal of Parallel and Distributed Computing*, vol. 187, p. 104848, 2024.
- [60] C. Zhang, J. Yang, M. Li, and N. Wang, "Reliability analysis of a two-dimensional linear consecutive-(r,s)-out-of-(m,n): F repairable system," *Reliability Engineering & System Safety*, vol. 242, p. 109792, 2024.
- [61] N. Mohamed, J. Al-Jaroodi, I. Jawhar, and A. Eid, "Reliability analysis of linear wireless sensor networks," in 2013 IEEE 12th International Symposium on Network Computing and Applications. IEEE, 2013, pp. 11–16.
- [62] Y. Mo, L. Xing, and J. Jiang, "Modeling and analyzing linear wireless sensor networks with backbone support," *IEEE Transactions on Systems, Man, and Cybernetics: Systems*, vol. 50, no. 10, pp. 3912–3924, 2018.

- [63] M. F. Carsancakli, M. A. Al Imran, H. U. Yildiz, A. Kara, and B. Tavli, "Reliability of linear WSNs: A complementary overview and analysis of impact of cascaded failures on network lifetime," *Ad Hoc Networks*, vol. 131, p. 102839, 2022.
- [64] C. Lin, L. Cui, D. W. Coit, and M. Lv, "Performance analysis for a wireless sensor network of star topology with random nodes deployment," *Wireless Personal Communications*, vol. 97, no. 3, pp. 3993–4013, 2017.
- [65] L. Chen, Y. Xu, F. Xu, Q. Hu, and Z. Tang, "Balancing the trade-off between cost and reliability for wireless sensor networks: a multi-objective optimized deployment method," *Applied Intelligence*, vol. 53, no. 8, pp. 9148–9173, 2023.
- [66] N. T. Boardman and K. M. Sullivan, "Time-based node deployment policies for reliable wireless sensor networks," *IEEE Transactions on Reliability*, vol. 70, no. 3, pp. 1204–1217, 2021.
- [67] ——, "Condition-based node deployment policies for reliable wireless sensor networks," in *Proceedings of the 2021 IISE Annual Conference*, 2021.
- [68] —, "Approximate dynamic programming for condition-based node deployment in a wireless sensor network," *Reliability Engineering & System Safety*, vol. 243, p. 109803, 2024.
- [69] F. Coolen and T. Coolen-Maturi, "Generalizing the signature to systems with multiple types of components," in *Complex Systems and Dependability*. Springer, 2013, pp. 115–130.
- [70] S. Reed, "An efficient algorithm for exact computation of system and survival signatures using binary decision diagrams," *Reliability Engineering and System Safety*, vol. 165, pp. 257–267, 2017.
- [71] S. Reed, M. Löfstrand, and J. Andrews, "An efficient algorithm for computing exact system and survival signatures of *k*-terminal network reliability," *Reliability Engineering & System Safety*, vol. 185, pp. 429–439, 2019.
- [72] B.-H. Xu, D.-Z. Yang, C. Qian, Q. Feng, Y. Ren, Z.-L. Wang, and B. Sun, "A new method for computing survival signature based on extended universal generating function," in 2019 International Conference on Quality, Reliability, Risk, Maintenance, and Safety Engineering (OR2MSE). IEEE, AUG 2019.
- [73] J. Behrensdorf, T.-E. Regenhardt, M. Broggi, and M. Beer, "Numerically efficient computation of the survival signature for the reliability analysis of large networks," *Reliability Engineering & System Safety*, vol. 216, p. 107935, dec 2021.
- [74] F. Di Maio, C. Pettorossi, and E. Zio, "Entropy-driven Monte Carlo simulation method for approximating the survival signature of complex infrastructures," *Reliability Engineering & System Safety*, vol. 231, p. 108982, MAR 2023.
- [75] D. B. Lopes da Silva and K. M. Sullivan, "An optimization-based monte carlo method for estimating the two-terminal survival signature of networks with two component classes," *Naval Research Logistics (NRL)*, Early View Online Version.

- [76] S.-T. Cheng and T.-Y. Chang, "An adaptive learning scheme for load balancing with zone partition in multi-sink wireless sensor network," *Expert Systems with Applications*, vol. 39, no. 10, pp. 9427–9434, 2012.
- [77] A. E. Abdulla, H. Nishiyama, and N. Kato, "Extending the lifetime of wireless sensor networks: A hybrid routing algorithm," *Computer Communications*, vol. 35, no. 9, pp. 1056–1063, 2012.
- [78] Y. Lin and Q. Wu, "Energy-conserving dynamic routing in multi-sink heterogeneous sensor networks," in 2010 International Conference on Communications and Mobile Computing, vol. 3. IEEE, 2010, pp. 269–273.
- [79] H. Asharioun, H. Asadollahi, T.-C. Wan, and N. Gharaei, "A survey on analytical modeling and mitigation techniques for the energy hole problem in corona-based wireless sensor network," *Wireless Personal Communications*, vol. 81, no. 1, pp. 161–187, 2015.
- [80] I. Azam, N. Javaid, A. Ahmad, W. Abdul, A. Almogren, and A. Alamri, "Balanced load distribution with energy hole avoidance in underwater WSNs," *IEEE Access*, vol. 5, pp. 15 206–15 221, 2017.
- [81] M. Finkelstein and J. Vaupel, "On random age and remaining lifetime for populations of items," *Applied Stochastic Models in Business and Industry*, vol. 31, no. 5, pp. 681–689, 2015.
- [82] D. C. Montgomery and G. C. Runger, *Applied statistics and probability for engineers*. John Wiley & Sons, 2020.
- [83] K. Deb, A. Pratap, S. Agarwal, and T. Meyarivan, "A fast and elitist multiobjective genetic algorithm: NSGA-II," *IEEE Transactions on Evolutionary Computation*, vol. 6, no. 2, pp. 182–197, 2002.
- [84] P. N. G. Bao, T. L. Quan, Q. T. Tho, and A. Garg, "NSGA-II: A multi-objective optimization algorithm," https://github.com/baopng/NSGA-II, 2017, accessed: 2023-03-22.

A Derivation of Equation 3

Let $p_u = \bar{F}((u+1)t')/\bar{F}(ut')$ denote the probability of transitioning from state $u = 0, 1, 2, ..., \infty$ into state u + 1, and note that state u transitions into state 0 with probability $1 - p_u$. We can derive the equation for limiting probabilities $\pi_u = \Pr(X = ut')$ by using the stationarity equations

$$\pi_u = \pi_{u-1} p_{u-1}, \quad u = 1, 2, \dots, \infty,$$
 (12)

and

$$\sum_{u=0}^{\infty} \pi_u = 1. \tag{13}$$

By recursively applying Equation (12), we have

$$\pi_{u} = \pi_{0} \prod_{j=0}^{u-1} p_{j} = \pi_{0} \prod_{j=0}^{u-1} \frac{\bar{F}((j+1)t')}{\bar{F}(jt')} = \pi_{0}\bar{F}(ut'), \quad u = 0, 1, \dots, \infty,$$
(14)

where the last equation follows (for $u \le 1$) because $\bar{F}(0) = 1$ and (for $u \ge 2$) due to cancellation of the numerator of the jth term in the product with the denominator of the (j+1)st term for $j=0,1,\ldots,u-2$. Substituting Equation (14) into Equation (13) for all $u=0,1,\ldots,\infty$ yields

$$\sum_{j=0}^{\infty} \pi_0 \bar{F}(jt') = 1, \tag{15}$$

which can be rearranged to solve for π_0 as

$$\pi_0 = \frac{1}{\sum_{j=0}^{\infty} \bar{F}(jt')}.$$
 (16)

By substituting Equation (16) into Equation (14), the remaining limiting probabilities are

$$\pi_{u} = \frac{\bar{F}(ut')}{\sum_{j=0}^{\infty} \bar{F}(jt')}, \quad u = 0, 1, \dots, \infty.$$
 (17)

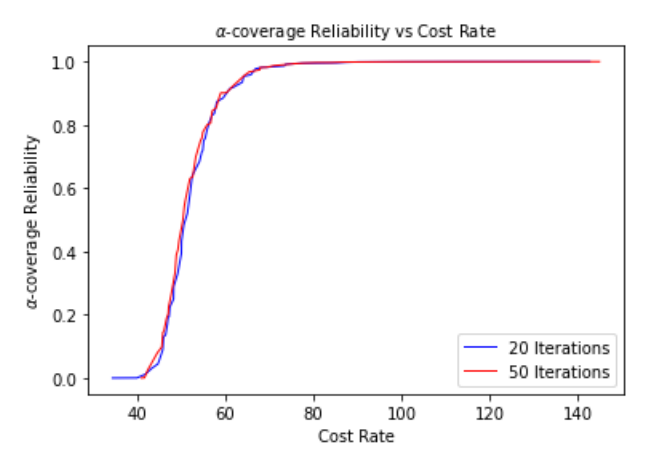


Figure 18: Number of Iterations vs Efficient Frontier

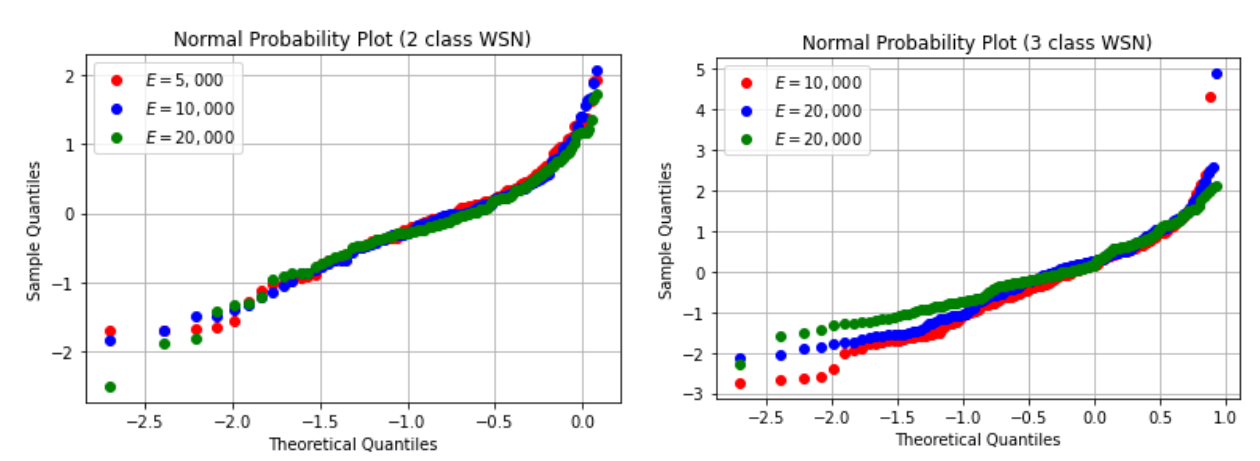


Figure 19: Normal probability plot (K = 2)

Figure 20: Normal probability plot (K = 3)

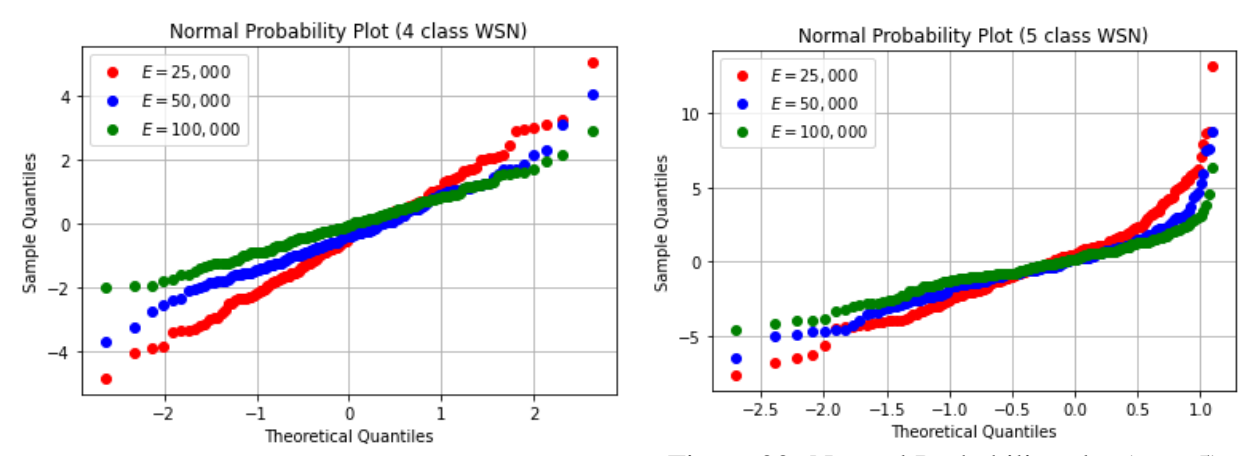


Figure 21: Normal probability plot (K = 4)

Figure 22: Normal Probability plot (K = 5)

B Efficacy of NSGA-II

We performed a convergence analysis to determine whether increasing the number of generations in NSGA-II might be likely to yield substantially improved solutions. For the instance with K = 4, we increased the number of generations from 20 to 50 and (due to time limitations), we set the initial population to 50 for both cases. All other parameters remained the same as described in Section 7.2. Figure 18 displays the efficient frontier for both cases. The results suggest that the increase in number of generations results in only very minor improvements in solution quality.

C Probability plot of W_q

Figures 19–22 show the normal probability plot for instances K = 2, 3, 4, 5 with respect to the W_q -values resulting from Equation (10).